THE PRODUCTION AND HUMAN INHALATION OF PLUTONIUM LABELLED PARTICLES IN THE SUB-MICRON RANGE

By

DAVID ALAN WAITE

Bachelor of Arts
Kansas State Teachers College
Emporia, Kansas
1963

Master of Science
Vanderbilt University
Nashville, Tennessee
1965

Submitted to the Faculty of the Graduate College
of the Oklahoma State University
in partial fulfillment of the requirements
for the Degree of
DOCTOR OF PHILOSOPHY
May, 1972

THE PRODUCTION AND HUMAN INHALATION OF PLUTONIUM LABELLED PARTICLES IN THE SUB-MICRON RANGE

Thesis Approved:

John B. Wedd
Thesis Adviser

J. K. Dorton

R. T. Lowery

O. D. Dunham
Dean of the Graduate College

ACKNOWLEDGEMENTS

To Dennis Ramsden who suggested to me the subject of this work and who supervised my research, I wish to express my sincere gratitude.

I also wish to thank Mr. H. T. Neville, Mr. Paul Foster, and Mr. Tom Johns for their invaluable experimental assistance.

For their continued support and sacrifice throughout my graduate studies I wish to thank Nancy, Michael, and Brian--my family.

To my committee, Dr. J. R. Norton, Dr. John West, and Dr. Richard Lowery, who cooperated in the unorthodox arrangements necessary for the conduct of this research, I would like to express my appreciation.

Finally, I wish to thank the United Kingdom Atomic Energy Authority for granting permission to conduct this research at the Winfrith Establishment and to use their copyrighted figures for this thesis.

...

TABLE OF CONTENTS

LIST OF TABLES

LIST OF FIGURES

CHAPTER I

INTRODUCTION

Although it was not generally recognized until several years afterward, the flourish of activity which followed Becquerel's discovery of radioactivity was accompanied by a hazard of internally deposited radioactivity equal to or of even greater importance than the external hazard of X-rays which was vaguely realized at the time. Either hazard was relatively small considering the population as a whole because of the insignificant number of people directly involved. However, since those times we have progressed through a period of limited though significant public utilization or availability to the present higher level of public utilization and exposure. This trend has followed the development of atomic energy from a laboratory phenomenon to a technique commonly used in education, government, medicine, and industry. Public involvement will most certainly accelerate with the installation of breeder type power reactors in populated areas because of the increased necessity for transcontinental or transworld shipments of irradiated fuel elements to plutonium extraction facilities. This point is illustrated by the following discussion.

The great practical importance of plutonium lies in its ability to undergo induced fission due to the absorption of neutrons and its ability to release a great amount of energy during the process.

The repeated use of plutonium, produced in a thermal reactor for

enriching fuel for the same reactor, permits a marked improvement in the use of natural uranium. Estimates indicate that the utilization of plutonium reduces the consumption of natural uranium to a level that seems feasible in light of the present data and estimates of uranium resources. The concise analysis of the present and future energy consumption in the world indicates a vital role for plutonium. Until large scale thermonuclear power stations are commissioned, the predominant role in the extension of the power industry will be played by U-238 or actually by plutonium which is produced from that isotope.

Taking as 100 the initial load of plutonium into the fast reactor, 20 parts of the plutonium are fissioned after one full cycle; at the same time 30 new parts of plutonium are formed. Thus after 10 fuel cycles an amount of plutonium equal to the initial load in the reactor is obtained. Plutonium is a fuel of greatest importance as far as the breeding process is concerned because of the relatively short time required for this doubling of the amount of fuel (approximately six years). It is evident, however, that the plutonium must be returned to the reactor several times before it can be completely utilized.

Many of the most common internally deposited fission products are handled routinely through whole body monitors. These products generally tend to emit X or gamma rays of 100 KeV or greater energy with relatively high yields, both of which make penetration of the human anatomy and detection fairly efficient. The isotope of particular importance here, Pu-239, unfortunately emits electromagnetic radiations of low energies and with relatively low yields. The production of U-235 through alpha decay of the Pu-239 of intensities 20, 70, 5.5, 2.5, and 1.5 quanta per million alpha transitions and by X-rays of 13.6, 17.4, and 20.5 KeV of

intensities 1.2, 1.3, and 0.3 x 10^{-2} quanta per decay.

As for the harmful effects of alpha emitting elements accumulated in the body, medicine has had the greatest experience with radium. During the past 60 years there have been cases of radium poisoning that often ended in death. The similarity between the physiological effects of radium and plutonium is due to the fact that both elements accumulate in bones in the form of insoluble phosphates, both emit alpha particles, and they have half lives differing only by one order of magnitude (radium--1540 years, plutonium--24,360 years).

The harmful effects of both radium and plutonium are increased substantially by the concentration mechanism in the body. Plutonium is absorbed by the tissues and is carried by the blood stream into the bones where it is accumulated. The critical organ for plutonium varies, however, depending upon the solubility of the material and upon the mode of intake. Bone is the only critical organ for inhaled, ingested, or injected plutonium in the soluble form. The lung is the critical organ for inhaled plutonium in the insoluble form. The gastrointestinal tract (GI tract) becomes the critical organ if insoluble plutonium is ingested. If the plutonium does eventually settle in the bone tissue and in the marrow cavity, the alpha particles emitted attack the blood-forming tissues directly.

On the basis of the above observations, it has been accepted that if an alpha emitting isotope concentrates in the bones like radium does, its toxicity can be compared to that of radium. The maximum permissible burdens for plutonium have been assessed by taking as a starting point comparable studies of toxicity of radium and plutonium in the bodies of animals. From this research it has been found that plutonium is much

more toxic than radium. The ratio of toxicities varies from 10 to 30 depending upon the duration of action on the body. In analyzing the past cases of radium poisoning, a maximum permissible body burden of 0.1 μCi or 0.1 μg of radium has been established. The maximum permissible body burden of plutonium is now established at 0.04 μCi (0.64 μg) which corresponds to approximately 1500 alpha disintegrations per second. Some calculations demonstrate how small the corresponding quantities of plutonium permissible in the atmosphere are. The maximum permissible concentration in air is 2×10^{-12} uCi/cm3, that is 3.2×10^{-11} μg/cm3, which means that air containing plutonium at the maximum permissible concentration must not have more than one plutonium particle of 0.1 μm diameter per liter.

Because all of these limits are based on the dose-effect relationship for irradiation of biological systems, one of the prime considerations in evaluating the potential hazards from internally deposited radioisotopes is the biological dose received by various organs. In such a determination the accurate estimation of the activity intake, A_o, is of paramount importance. Since reconstruction of acute intake circumstances is not often possible, the only alternative solution to the problem is the estimation of A_o after the fact by any measure available.

The measures which are available would be better if it were not for the fact that each inhalation and victim is physically and physiologically different. Errors are induced in all forms of counting data by such physical differences. Bioassay error is induced by physiological differences. What is needed, therefore, is a set of data correction factors involving these physical and physiological variables. The raw counting or bioassay data could then be treated with these factors to

yield an accurate estimate of A_0. Attempts are presently being made to achieve this goal, but possible results are limited because of the restriction of related research to laboratory animals or to human phantom studies.

In 1967 Ramsden and Davis analyzed the calibration errors which exist in phantom-related work and subsequently proposed experiments to minimize these errors. It was proposed at that time that a very limited number of experiments be carried out using human volunteers inhaling an aerosol of known activity, solubility, and particle size. Data from the volunteers would be collected over a definite period of time by enough independent means to indicate both levels and trends concerning aerosol retention, excretion, translocation, and distribution.

It was decided at a much later date that the most efficient implementation of these objectives would necessitate the orderly development along the following lines: (a) development, construction, and testing of a suitable aerosol generating apparatus; (b) production and extensive investigation of properties of a suitable aerosol; (c) sequential inhalations by a single volunteer of aerosol tagged first with a soluble form of a gamma emitting isotope and then with an insoluble form of the same isotope with subsequent compilation of data on the retention, excretion, and distribution of the inhaled material; and (d) inhalations by two volunteers of aerosol tagged with the insoluble form of an isotope which emits both X-rays in the 13-22 KeV region and gamma rays in the 100-400 KeV region using a one-deep-breath-and-hold breathing pattern in one case and shallow, continuous breathing in the other with the same data being taken as in the previously mentioned inhalations.

The experiments which will be discussed in this thesis are based

on the previously mentioned objectives. The first step (a) was achieved by constructing and testing an apparatus for producing insoluble spherical aerosol particles in the range 0.1 to 0.5 μm. This method is extremely well suited to the case when the available material for nebulizing is limited and gives an overall recovery efficiency of 25%. The resultant particles are discrete, insoluble, and spherical but give a density which varies rapidly with particle size. The apparatus can be easily adjusted to give a high yield of particles of any chosen size in this range. The lower limit of particle size would appear to be of the order of 0.01 μm.

The method of generating insoluble iron oxide aerosols in the size range 0.1 to 0.5 μm, giving hollow particles of low density, can be applied to human volunteer inhalations while retaining the high efficiency of aerosol production. The leaching characteristics of the tagging isotope, which depend critically on the particle size and the chemical form of the radioactive label, can be determined by *in vitro* studies. The results of such inhalations give a consistent pattern of lung deposition and biological excretion, showing a high lung retention with a long, retained half period for a typical breathing pattern aimed at maximizing pulmonary deposition. Such deposition and retention curves can be corrected for the leaching characteristics of the tagged isotope and expressed in terms of retained aerosol when conditions of high leaching *in vivo* exist.

CHAPTER II

HISTORY

The history of plutonium is short in terms of years, but its role in the modern world is of great significance. The plutonium isotope Pu-238 was discovered in 1940 and this discovery was followed shortly by the discovery of the more easily fissioned isotope Pu-239. Utilization of Pu-239 as a source of nuclear energy proceeded rapidly, and, consequently, plutonium production soon became an important industry. Out of scientific and political necessity, early plutonium experimentation and experience went through phases of biologically sterile investigations of physical and chemical properties to analytical methods and their applications. However, prior experience with radium poisoning, which had occurred in radium watch dial painters and others who had received radium either occupationally or therapeutically, had resulted in an awareness of biological hazards of exposure to radioactive materials in general. The post-war acceleration of free publication of plutonium data began to contain biological hazards in the early 1960's.

Injection Studies

Extensive work of the Utah group and others (1, 2, 3) provided studies of intraperitoneally and intravenously administered soluble compounds of plutonium. Studies of the metabolism and toxicity of Pu-239 in small laboratory animals were initiated in an effort to assess

its potential role as an industrial hazard. The basic concept employed was to determine the relative toxicities of Pu-239 and Ra-226 in mice, rats, and rabbits; then to use this information, the knowledge of the effects of Ra-226 in man and the observed differences in human and rodent metabolism of the two radionuclides, to estimate the effects of Pu-239 in man.

Although large numbers of animals had been used, as well as several criteria of toxicity, there, nevertheless, existed a great need for additional laboratory studies on animals which have longer lifespans than rodents and which have skeletons more like those of man. The reasons for this were as follows: (a) Some of the principal effects observed in human radium poisoning are bone tumors, spontaneous bone fractures, carcinoma of the paranasal sinuses, and other more subtle skeletal changes. (b) Studies with Pu-239 in rodents indicated that it might produce bone tumors in man. (c) The times required for these effects to become manifest are about 15 to 20 years in man and the major portion of lifespan in rodents. (d) Since only adults would risk industrial exposure to Pu-239, knowledge was needed of its effects when deposited in a mature skeleton in contrast with a continuously growing rodent skeleton.

Inhalation Studies

Short term effects, following injection or inhalation, relating plutonium excretion, retention, tissue distribution, and dose were also found to be very important. The pioneering investigations of Scott, Abrams, and their co-workers (4, 5), which included work on plutonium fumes and smokes, were effective in pointing out the general

behavior of plutonium aerosols in biological systems. Studies by Bair and his co-workers (6), which are based primarily on insoluble forms of plutonium, are perhaps more pertinent presently.

Using inhalation as the mode of administration and Beagle dogs as the experimental animal, Bair has produced a large fraction of present knowledge concerning inhalation of insoluble aerosols. His experimental objectives have been to investigate the fate of plutonium taken into the body with inspired air. This information is required to evaluate the potential hazards of breathing air contaminated with plutonium and to aid in the establishment of permissible limits. Specifically required are knowledge of the fraction of plutonium inhaled that is deposited in the respiratory tract and the duration of its residency at the sites of deposition and in other tissues where plutonium is translocated. This information is helping to identify the tissues irradiated and to indicate the dose delivered. Knowledge of the relationship between body burden of plutonium and levels in blood and excreta are aiding in evaluating personnel exposures, because plutonium is not easily detected by external counting procedures.

Similar experiments investigating the deposition and the fate of deposited plutonium as a function of particle size and of the total amount of plutonium deposited showed a marked effect of particle size on clearance, translocation, and excretion. Since comparisons of early animal results involved injection studies, experiments were completed to compare the behavior of inhaled and injected plutonium with the following results: (a) For inhaled aerosols the pulmonary clearance process was found to be describable as a multiphasic exponential. (b) The bronchial lymph nodes and the lungs have the highest plutonium

concentration and on the average account for 95% of the body burden. (c) Few extrapulmonary tissues except the gonads and lymph nodes appear to receive important radiation doses.

Human Studies

Human data which are available have been collected primarily from accidentally exposed individuals. Langham (7) did conduct a Pu-239 injection experiment using sixteen terminal human patients. This study still provides much of the most useful data on the subject.

The most comprehensive compilation and analysis of animal and human data on inhaled aerosols is the Task Group on Lung Dynamics publication (8). With the ultimate objective of translating all available data into useful and applicable concepts, this group has provided a great service which would not have been possible by any other means. The ready availability of this data with the relevant conclusions and models has made it possible to standardize related research results which may be human, phantom, or laboratory-animal based (9, 10).

It is obvious, however, that much remains to be done before plutonium inhalation severity can be accurately assessed through the extrapolation of animal data, through bioassay data, or through phantom-calibrated whole body or lung monitor results. The limitation of the last alternative method is the absence of the necessary phantom calibration to a human standard which should precede any human calibration to a phantom standard. Even though much progress has been made on the design and fabrication of human phantoms many of the same problems that inhibit accuracy in animal data extrapolation also limit accuracy in phantom-to-human extrapolations.

Long involvement in this field of study led Dautrebande (11) to express his concern over the data available at that time, and to a large extent his statements are still true. He notices that many conflicting results had been published regarding the deposition of airborne particulates in the respiratory tract. Most of the studies, relating either the mass or number of particles deposited in the lungs, had produced exaggeratedly scattered results, i.e., from 25% to 90% for mass and from 15% to 50% for the number deposited. Among the many factors which he says have contributed to this situation are the omission of consideration of such important inhalation aspects as: changes in particle size distribution with changing solute concentrations as solutions are dispersed with some nebulizers, breathing methods and conditions, the duration of the breathing pause at the peak of the inspiratory phase, and the respiratory frequency and depth.

Equipment

As important as the above to the successful conclusion of an inhalation experiment are the selection, operation, and reliability of the aerosol production equipment and detection methods for the deposited aerosol material.

Atomizing devices commonly used in generating aerosols may be classified into three main types. The first is the air blast or aerodynamical atomizer in which compressed air or other gas is used at high velocity to break up liquid emerging from a nozzle. It is characteristic of atomizers of this type that they give a very wide range of droplet size though in some cases this variation is reduced by trapping the larger droplets within the atomizer.

The second type depends on centrifugal action, the liquid being fed onto the center of a rotating disc, cone, or top and centrifuged off the edge. The spray is characterized by uniformity of the main droplet size in marked contrast to the heterogeneity of sprays produced by most other methods.

Thirdly, there is the hydraulic or hydrodynamical type in which liquid is forced through a nozzle and breaks up into droplets. Here the disintegration depends more upon the physical properties of the liquid and the conditions of ejection from the nozzle than upon interaction between the liquid and the surrounding gas. Probably the most successful hydraulic atomizer, and indeed the only one which has application for fine atomization, is the swirl chamber atomizer used in agricultural spraying equipment, internal combustion engines, and gas turbines. The swirl is produced by leading the liquid tangentially into the chamber and allowing it to spray out through a central orifice of small diameter.

Outside this classification, and very much less well-known, are two additional types which may be listed as special atomizers. These are the electrostatic atomizers which break up liquid by the action of electrostatic forces and the acoustic atomizer which utlizes high intensity sonic or ultrasonic vibrations. It is such an ultrasonic device which is used to produce all of the particles which will be used in this project. The prototype of this type of nebulizer was first described in 1927.

A vast number of different materials have been used as the primary constituent of aerosol particles. These include everything from India ink to human serum albumin and polystyrene to iron oxide (12, 13). Iron oxide was selected as the aerosol material to be used in this project.

Detection of the radioactively labelled aerosol particles once they are deposited in the lung can be based on whole or partial body counting techniques or on excretion studies or occasionally on examinations of tissues or tissue fluid samples. Whole body radioactivity monitors vary considerably in design, but all are proposed for the assessment of low level radioactive body burdens in man (14). In a majority of cases these monitors consist of a steel room acting as a radiation shield, a very sensitive detector system, and a subject support that provides a constant monitoring geometry. Whole body monitor measurements are adequate to detect incorporated activities at or below permissible levels for a very substantial number of nuclides, whether the levels taken are those that apply for single intakes or for a continuing intake at a constant rate. Partial body or local counting of the activity of a particular area of the body gives not only the extent of internal contamination but can also indicate isotope location and distribution.

Measurements of the excretion rate of radionuclides in the urine or feces are generally profitable for nuclides of which the permissible retained activities are low or the radiations are weakly penetrating. These advantages are achieved because of the removal of the absorbing medium and of the activity concentration steps which are the outstanding characteristics of all bioassay procedures.

It was the evaluation, in terms of the equipment and methods described, of various omissions of previous inhalation work as they apply to operational health physics which led to the establishment of the experiment objectives which will be discussed in the next chapter.

CHAPTER III

PROJECT OBJECTIVES

Since the early days of the radiation era, it has been recognized that maximum benefits could be derived from ionizing radiation uses only if the individuals directly involved were physically and psychologically safe in their occupational pursuits. Practical and experimental determinations of what practices are or are not safe usually result in the establishment of standards or limits which are designed to effect both individuals and their tasks in such a way that neither will be predicted to suffer adverse consequences in the light of present experience and knowledge. In order to have the maximum effect, however, these limits must be accurately appraisable with presently available instrumentation, personnel, and techniques. Unfortunately, the evaluation of Pu-239 internal deposition, limited by the Maximum Permissible Body Burden, involves several intrinsic variables which tend to eliminate it from the limit group of maximum effect.

Because all limits in radiation dosimetry are based on the dose-effect relationship for irradiation of biological systems, one of the prime considerations in evaluating the potential hazards from internally deposited radioisotopes is the biological dose received by various organs. From the equation

$$D_c^t = 51.1 \left(\frac{A_o f_w}{\lambda_{eff} M}\right) \Sigma EF\ (RBE)n \times (1-e^{-\lambda_{eff} t})$$

where D_o^t is the dose equivalent in rem received by an organ from time t = 0 to t following an acute intake, A_o is the activity of nuclide deposited in microcuries, f_w is the fraction of the nuclide deposited which reaches the organ of reference, λ_{eff} is the effective decay constant which considers both physical decay and biological elimination, M is the mass of the organ in grams, and $\sum$ EF (RBE)n is a constant related to the damaging effect per disintegration, it can be seen that the accurate determination of A_o is of paramount importance since it is the only variable that is not independently determinable. If A_o is not known, then D_o^t cannot be calculated, no comparisons to specified limits can be made, and no definite mode of corrective reaction, if necessary, can be formulated in behalf of the individual involved.

Historically, the inhalation or ingestion cases were of the chronic intake variety. Evaluation of total intake from chronic exposure can be conveniently evaluated because the intake circumstances are usually well known and can be readily reconstructed if they do not still exist. More recently the major concern of internal dose evaluation units has been acute inhalation victims. In these circumstances A_o is the main unknown variable and usually accurate reconstruction is not possible. The only alternative solution to the problem is the estimation of A_o after the fact by any measure available. Common techniques used for this lung burden estimation were discussed in the last chapter.

These methods would be better if it were not for the fact that each inhalation and victim is physically and physiologically different. Errors are induced into all forms of counting data by such physical differences. Bioassay error is induced by widely varying isotope solubilities and by different individual excretion rates and patterns. What

is needed, therefore, is a set of data correction factors involving physical and physiological variables. The raw counting or bioassay data could then be treated with these factors to yield an accurate determination of A_o. Attempts are presently being made to achieve this goal, but possible results are limited because of the restriction of related research to laboratory animals or to human phantom studies.

The first publication of work at the Atomic Energy Establishment, Winfrith, England, in this area was in 1962 (15). By 1967 several important contributions to the effort of detecting Pu-239 in vivo had been made by the group (16, 17, 18). In this year Ramsden and Davis (19) analyzed the calibration errors which exist in phantom-related work and subsequently proposed experiments to minimize these errors. Even with the progress which had already been made they concluded that two main sources of error remained, the magnitudes of which were unknown but which might well be large. These were systematic errors in the chest phantom and errors stemming from the distribution of the contaminant throughout the chest.

In the early stages of the work it became apparent that a large systematic error was caused by a gross mismatch of the soft tissue thickness overlying the ribs between normal individuals and the chest phantom. Ultrasonic studies of the soft tissue thicknesses on the chests of a group of individuals of widely varying body build gave them confidence in being able to predict a mean soft tissue thickness of any individual to within 2 mm. Without such a correction any answers obtained by measuring the plutonium K X-rays would be in error by as much as a factor of 4. It was found to be conceivable that other sources of systematic error also existed in the phantom. Among them were the

relative thickness of fat and muscle tissue in the chest, the differences in soft tissue thickness beneath the rib cage, the rib thicknesses and relative spacings, and the size and shape of the lungs. The phantom was constructed to be a good match to a living subject at X-ray energies above 10 KeV. However, at best, it is only a simulation of a "standard man," and a series of cross calibrations between individuals and the phantom would be invaluable.

Any variation in distributions was not allowed for in the phantom calibrations, which are based on an assumed homogeneous distribution of activity throughout the lung. As the detection technique depends on counting soft X-rays ($\tilde{}$ 17 KeV) which are readily absorbed in soft tissue (half thickness $\approx$ 0.6 cm of soft tissue), slight changes in distribution throughout the chest region could produce large differences in observed counting rates. It is known that the distribution of activity varies with time as large particles are rapidly cleared by ciliary action, and small ones are only slowly trapped in the lymphatic system. The distribution in any incident obviously depends on several factors, the following of which they hoped to study in the proposed experiments: (a) the spectrum of particle sizes inhaled, (b) the relative solubility of the particles in the chest and the ease of movement of the very small particles throughout the lung, (c) the physiology and history of the individual involved.

It was proposed at that time that a very limited number of experiments be carried out using human volunteers inhaling an aerosol of known activity, solubility, and particle size. So little is known of the distribution of activity in the lung following an inhalation incident that a considerable program of work could be started in this field by varying

some of the many parameters involved, such as particle size; particle solubility; inhalation period, i.e., one breath or continual breathing; and depth of breathing.

Two basic experimental approaches appeared to be possible:

1. Labelling monodispersed aerosols of known particle size with easily identifiable gamma emitting isotopes. The inhalation of such aerosols would enable the distribution of activity throughout the chest to be determined thus resolving the distribution problems discussed previously.

2. Labelling the aerosol with isotopes that emit soft X-rays similar to those of Pu-239 (13.6, 17.0, 20.4 KeV). The volunteer subjects would then be counted directly with the detectors developed for the estimation of Pu-239 in vivo. This approach would resolve the systematic errors present in the phantom but would give little indication of the distribution of activity in the chest due to the absorption and scattering of the X-rays in body tissue.

A combination of both approaches would be obtained if isotopes were used which emitted both easily identifiable gamma rays and suitable X-rays.

At a much later date it was decided that the most efficient implementation of these objectives would necessitate the orderly development along the following lines:

1. Development, construction, and testing of a suitable aerosol generation apparatus.

2. Production and extensive investigation of properties of a suitable aerosol.

3. Sequential inhalations by a single volunteer of aerosol tagged

first with a soluble form of a gamma emitting isotope and then with an insoluble form of the same isotope with the subsequent compilation of data on the retention, excretion, and distribution of the inhaled material.

4. Inhalations by two volunteers of aerosol tagged with the insoluble form of an isotope which emits both X-rays in the 13-22 KeV region and gamma rays in the 100-500 KeV region using a one-deep-breath-and-hold breathing pattern in one case and shallow, continuous breathing in the other with the same data being taken as in the previously mentioned inhalations.

These specific topics will be dealt with individually and in detail in the following chapters.

CHAPTER IV

THE PRODUCTION OF EXPERIMENTALLY LABELLED AEROSOLS IN THE SUB-MICRON RANGE

Studies of lung retention, sites of deposition, relocation and clearance following the inhalation of aerosols are in progress at several centers throughout the world (8, 20-23). As part of studies concerning the behavior of insoluble particles in the lung, with an aim to improving the ability to detect and estimate Pu-239 lung burdens in man, there is interest in producing insoluble particles in the size range 0.05 to 0.5 μm and in tagging such particles with relatively short half life "non-leachable" radioactive label in order to study their behavior in vivo (24, 25). Of the labels being used, some are cyclotron produced and only available in small quantities [e.g. Pu-237 ($t_{\frac{1}{2}}$ 43 days)].

Most of the aerosol generators and work reported in the literature produce particles in the size range 1 to 20 μm, and the generators have a low efficiency of nebulization, i.e., only a small fraction of the original material is finally available as aerosol, and of this only a small fraction is actually inhaled. In order to handle the limited quantities of materials available, an overall efficiency of about 20% from the initial isotope production on the cyclotron to the final retained lung fraction was necessary with particles of the order of 0.1 μm diameter and a fairly homogeneous size distribution.

Of the types of generator available, the ultrasonic nebulizer appeared the most promising. Particles produced by such a method show high porosity, and some trouble from the leaching of the radioactive label was expected (26). However, such a generator under the proper conditions will operate at high nebulizing efficiency.

An aerosol production apparatus built around such a nebulizer was constructed and tested. Specifically designed to operate at high efficiency and low air volume, the apparatus is ideally suited for work with aerosol particles tagged with less readily available isotopes. To overcome the severe efficiency losses which accompany the often used nebulize-precipitate-dehydrate-suspend-renebulize sequence of stable aerosol production, the device incorporates the particle dehydration essentials in the inlet air drying and preheating sections.

Basic Technique

The aerosol particles are dehydrated ferric oxide (Fe_2O_3) and are produced by nebulizing an aqueous deionized iron sol which is prepared in a manner very similar to that of Albert and his co-workers (27). The sols are prepared from ferric chloride and ferric nitrate solutions, deionization being of the order of 93% and iron concentrations varying up to a maximum of 1.5%.

The addition of the radioactive label (tag) is done in the sol phase prior to nebulization. The efficiency of labelling and the stability of the tag both *in vivo* and *in vitro* depend on the method of production of the sol, the chemical form of the isotopic tag, and the pH value of the mixture. With optimum conditions a labelling efficiency of greater than 90% can be obtained for many isotopes without any dele-

terious effects on either the sol or the subsequent aerosols. The sols prove to be very stable and can be stored for long periods both in the tagged or untagged state.

Nebulization of the sol produces droplets which, when dry, give hollow spheres of dehydrated ferric oxide. The method of production and the particle characteristics are described below.

Apparatus Construction

The apparatus, shown schematically in Figure 1 and photographically in Figure 2, consists of an aerosol generation box and aerosol storage reservoir. The four liter generation box is constructed in three sections of square cross section, each of which is detachable for decontamination and internal modification purposes.

Section 1, the heating chamber, consists of a conventional light bulb and socket mounted in a square box of 1/16th inch aluminum.

Section 2, the ultrasonic nebulizer, originally manufactured for use in the humidification of inspired gas for patients with tracheostomy or an endotracheal tube, is located at the base of the nebulizing chamber (28). In order to make the air movement as uniform as possible in this chamber, baffle plates are inserted between it and the heating chamber. The design of these baffles was empirical, most of the slots being at the sides and base of the plates.

Section 3, the electrostatic precipitator, consists of four polished steel plates with staggered holes cut so as to ensure a maximum path length for the air stream without producing direct impingement onto the perspex container walls. In practice this precipitator was not required for its initial purpose and served merely to provide a long

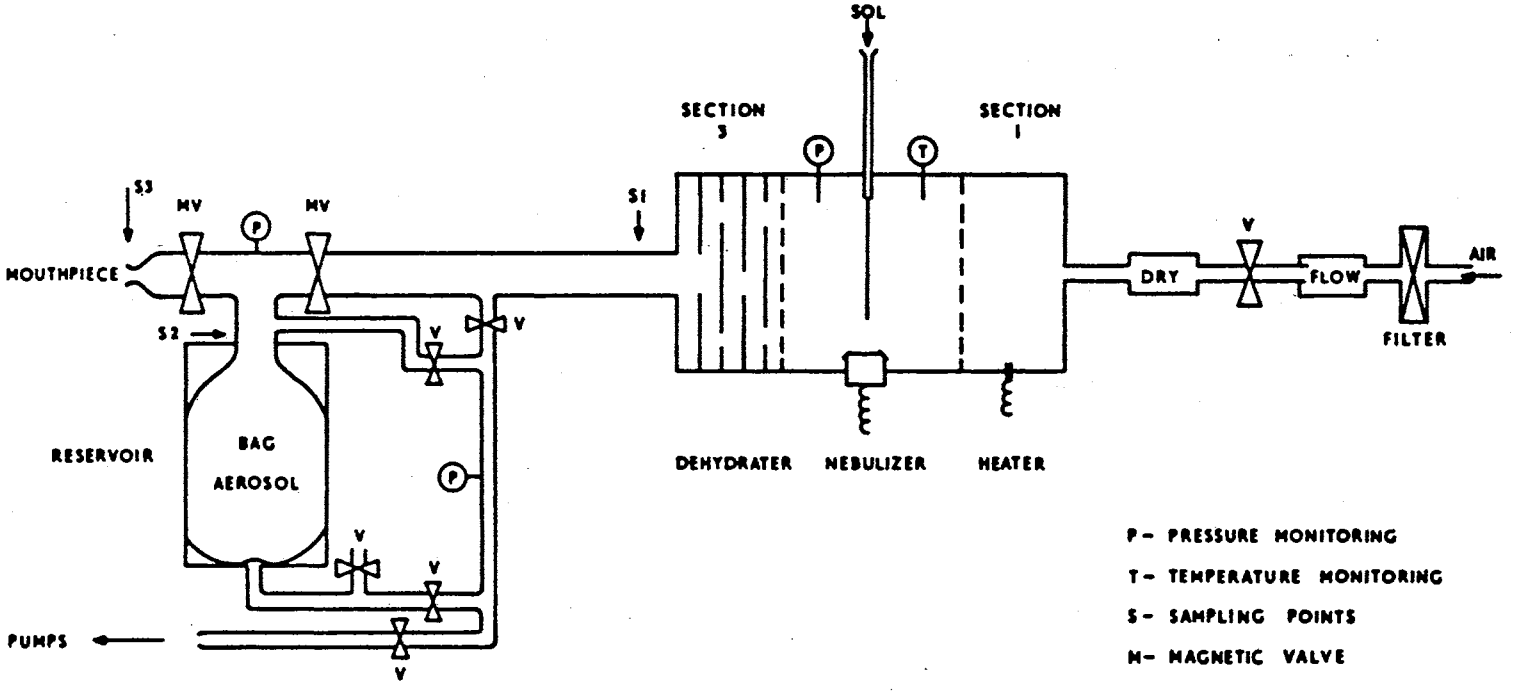

Figure 1. Schematic Block of Generation Apparatus

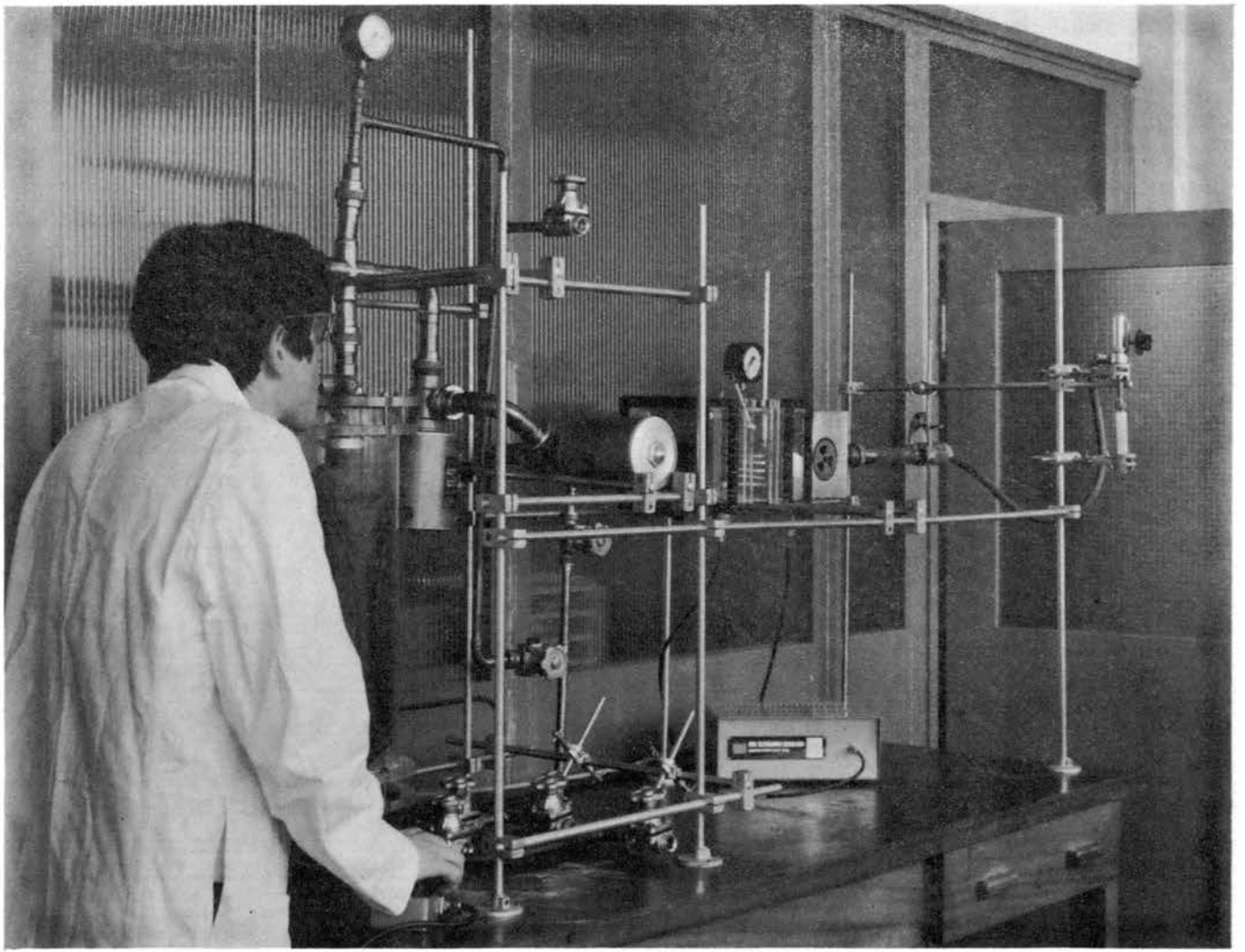

Figure 2. Aerosol Generation Apparatus

drying path for the air stream to ensure complete drying of the original droplets.

Both Sections 2 and 3 are constructed of 1/8th inch perspex with gasketed flanges and conventional clamping. Pressure and temperature can be monitored at several points as can flow rates and volumes. Facilities are also available to extract samples of the aerosols at several points. This sampling is usually onto Millipore papers (0.01 μm).

The aerosol reservoir consists of a $\frac{1}{4}$ inch perspex cylinder, 6 in. diameter by 18 in. long, containing an eight liter veterinary cattle anesthetic bag which is attached to the main airstream line. The bag and the rest of the cylinder can be independently evacuated to enable pressure balancing to be done before inhalation. On Figure 1 the main aerosol lines (1 inch copper) and vacuum or control bypass lines ($\frac{1}{2}$ inch copper) are also shown. The arrangement of the bypass lines ensures that proper pressure, temperature, and flow rate conditions are established before the aerosol is produced. The bag is initially evacuated and filled during nebulization. Pressure balancing is achieved by independently controlling the bypass lines into the perspex cylinder.

Aerosol Production

The filtered inlet air moves at approximately eight liters per minute into a silica gel drying tube. The dry air is then heated to about 40°C in the heating chamber by a 60-watt light bulb. The final stability of the particles is very dependent on the proper conditions being maintained in these two areas, i.e., a controlled flow of warm, dry air.

The sol is introduced into the nebulizer from a calibrated syringe

set into the roof of the nebulizer chamber (Section 2). The size of the droplets produced is primarily determined by the frequency and power of the crystal and is 3 /um for the particular 3 MHz crystal used.

Dehydration of the droplets takes place mainly in the electrostatic precipitator (Section 3 of Figure 1). Testing of particles collected at point S1 of this figure shows that the particles are completely dehydrated and stable in aqueous environments.

From the dehydration chamber the aerosol is collected into the reservoir. Storage times of up to two hours in the bag have little effect on the particle recovery from the bag or on the size distribution.

Inhalations are done directly from this bag via a normal anesthetic mouthpiece. The subject controls his own inhalation by means of magnetic valves, switching from normal laboratory air to the reservoir. The exhaled fraction is recollected in the bag which is externally monitored by a scintillation detector. The bag is finally completely evacuated through Millipore filters.

Efficiency of Nebulization

Although efficiency is discussed in this section and particle size later in the chapter, it should be pointed out that the two are interrelated.

As mentioned above, the main objective was to obtain a high reproducible overall efficiency. The tests of efficiency were done using radioactive labels [Fe-59 ($t_{\frac{1}{2}}$ 45 days), Cr-51 ($t_{\frac{1}{2}}$ 27 days)] and counting samples of the filtered aerosol from several points in the apparatus. Further tests showed that these samples consisted of dry, discrete, spherical particles of ferric oxide which could easily be

resuspended from the Millipore papers and studied under an electron microscope. A known initial activity was introduced into the nebulizing chamber as a small volume of labelled sol and all efficiencies obtained refer back to this initial activity as a percentage collected. Testing at the aerosol exit (Point S3 of Figure 1) showed no statistical difference in collection efficiency here and at Points S1 and S2.

Nebulization efficiency was studied as a function of: (a) sol concentration, (b) flow rate, (c) collection time, (d) back washing, and (e) sol volume. The results are presented graphically in Figures 3-6.

The efficiency, as a function of sol concentration, is shown in Figure 3 with the 1σ confidence interval noted. Within the statistics shown, very little trend can be deducted from this graph. There is evidence of a broad maximum in efficiency of 25% with sol concentrations of about 0.1% iron by weight. Certainly at higher concentrations, giving larger particle sizes, increasing loss due to impaction may be expected. The drop in efficiency at lower concentrations (smaller particle size) is attributed to the apparatus design.

Figure 4 shows the continuously improving efficiency with flow rate throughout the workable flow rate range (sol concentration was kept at 1.5% iron).

Figure 5 shows the relationship between collection efficiency and collection time for a 1.5% iron sol being collected at eight liters per minute. All three graphs show that a mean efficiency of 25% is easily obtainable with usable flow conditions. A standard flow rate of eight liters per minute at a reduced pressure of 2/3 of atmospheric and a collection time of one minute gives a stock aerosol volume which can be

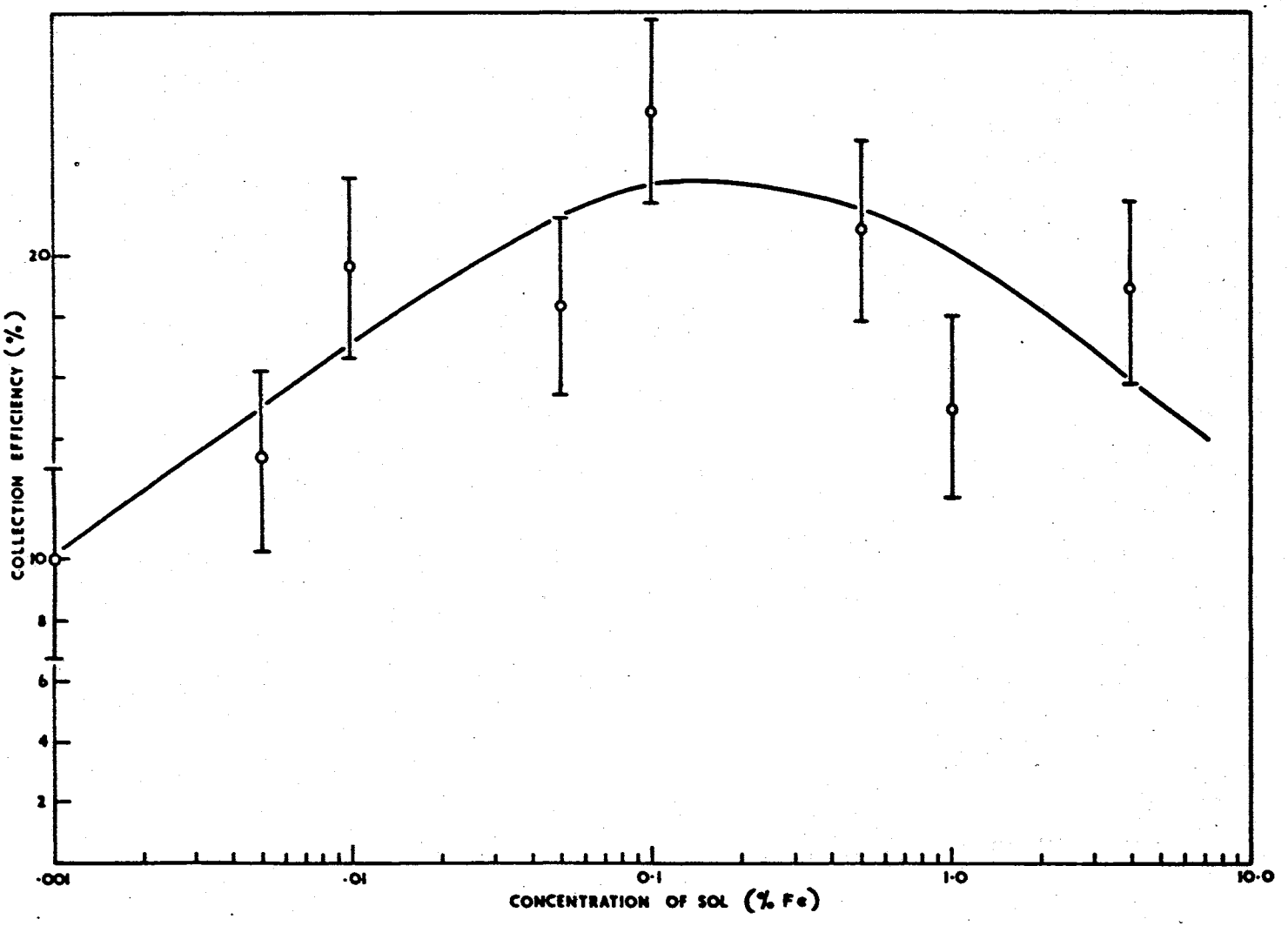

Figure 3. Particle Collection Efficiency vs. Sol Concentration

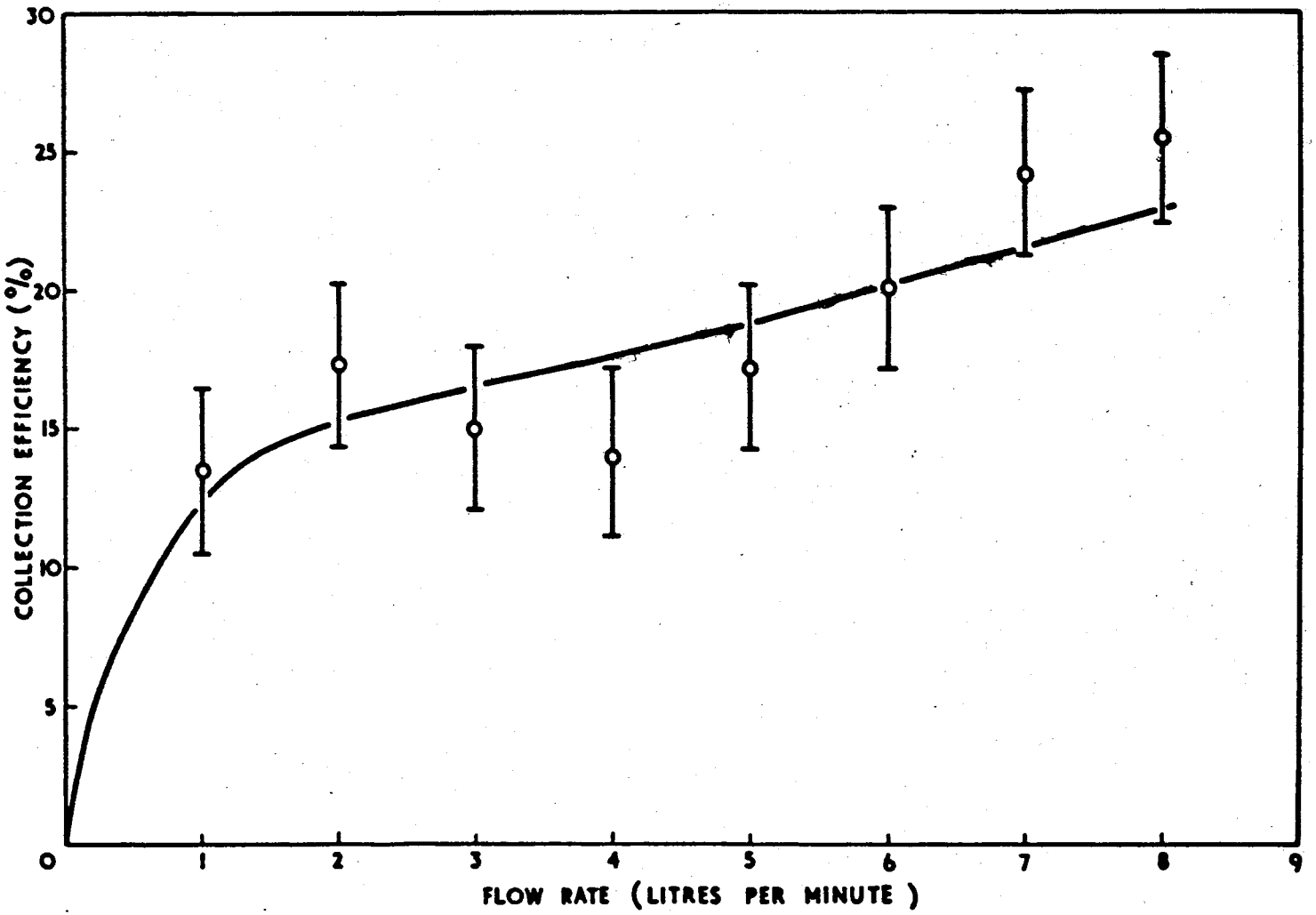

Figure 4. Particle Collection Efficiency vs. Collection Flow Rate

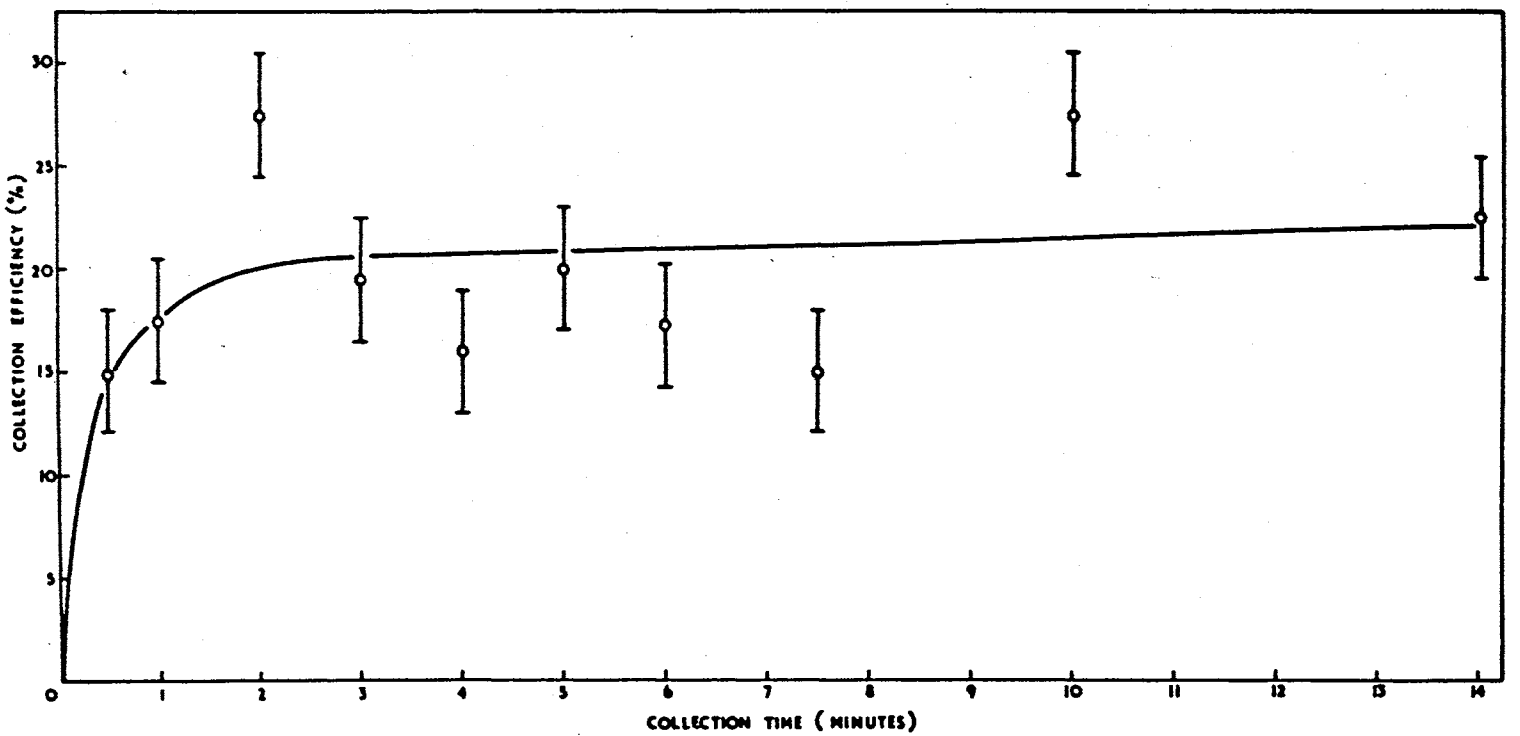

Figure 5. Particle Collection Efficiency vs. Collection Time

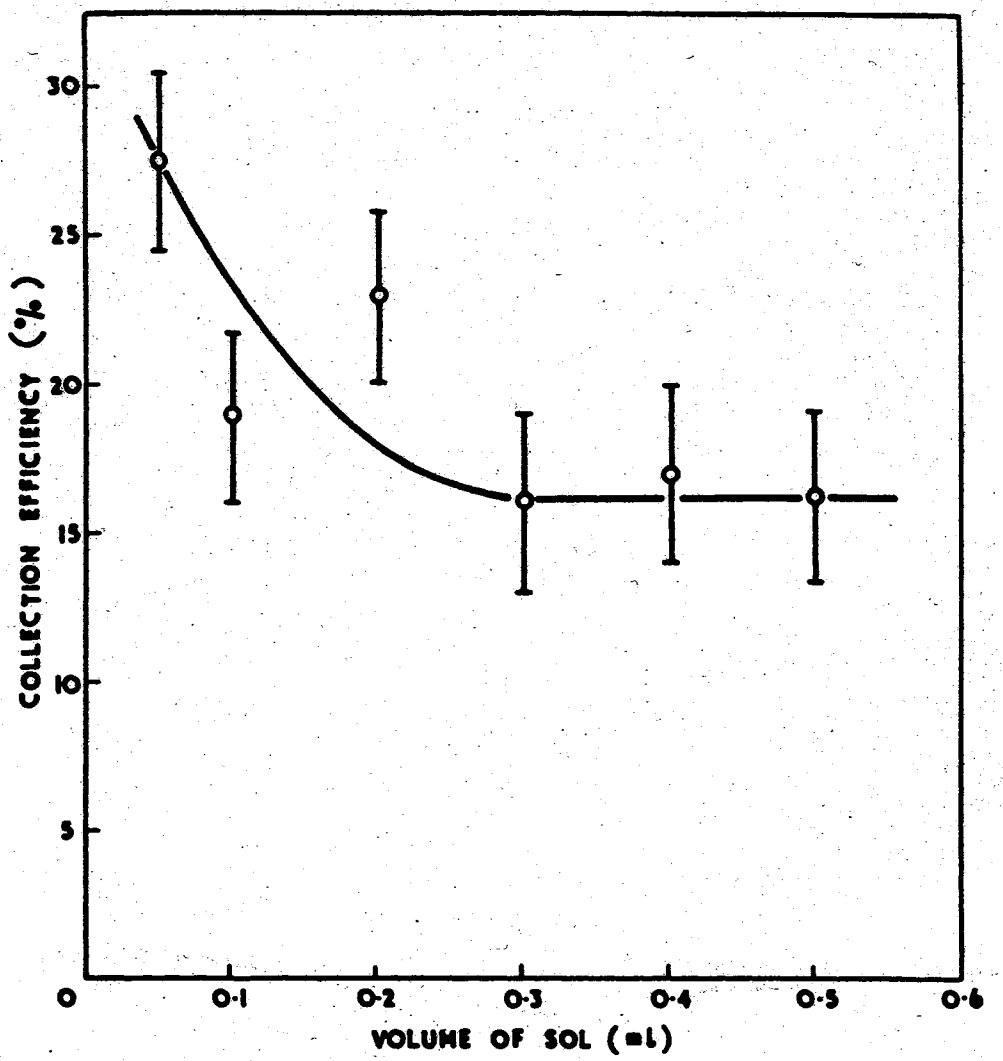

Figure 6. Particle Collection Efficiency vs. Sol Volume

inhaled in one or two breaths.

Efficiency can be improved still further if an attempt is made to wash back some of the settling droplets and splashes which occur in the nebulizing chamber. The loss due to "splashing" (about 50%) from the crystal is a function of the initial volume of sol introduced. Large volumes of sol also increase the humidity beyond the capability of the heating and drying system. Figure 6 shows the increase in efficiency with reducing the sol volume. At these small volumes (0.1 ml) losses in the capillary syringe become important and if a small washing volume is introduced the efficiency can be increased further. This step, however, tends to dilute the last stages of nebulization and produces an aerosol with a larger than normal proportion of small particles.

Collection efficiencies are relatively independent of differential pressure or of air temperature once favorable dehydration conditions have been established.

Particle Characteristics

Examination of the physical characteristics and particle sizing were done using stereoscan micrographs produced on a scanning electron microscope. Figure 7 shows that the particles have the desired spherical shape and are not aggregated. If complete dehydration is not achieved, an aggregate of platelets is seen; these are not stable in aqueous environments and revert back to the solution.

Particle sizes taken from these micrographs exhibit a normal distribution (Figure 8), the count median diameter (CMD) being a function of the iron concentration in the sol (Figure 9). Assuming that the final aerosol particle results from simple dehydration of the 3 μm sol droplet

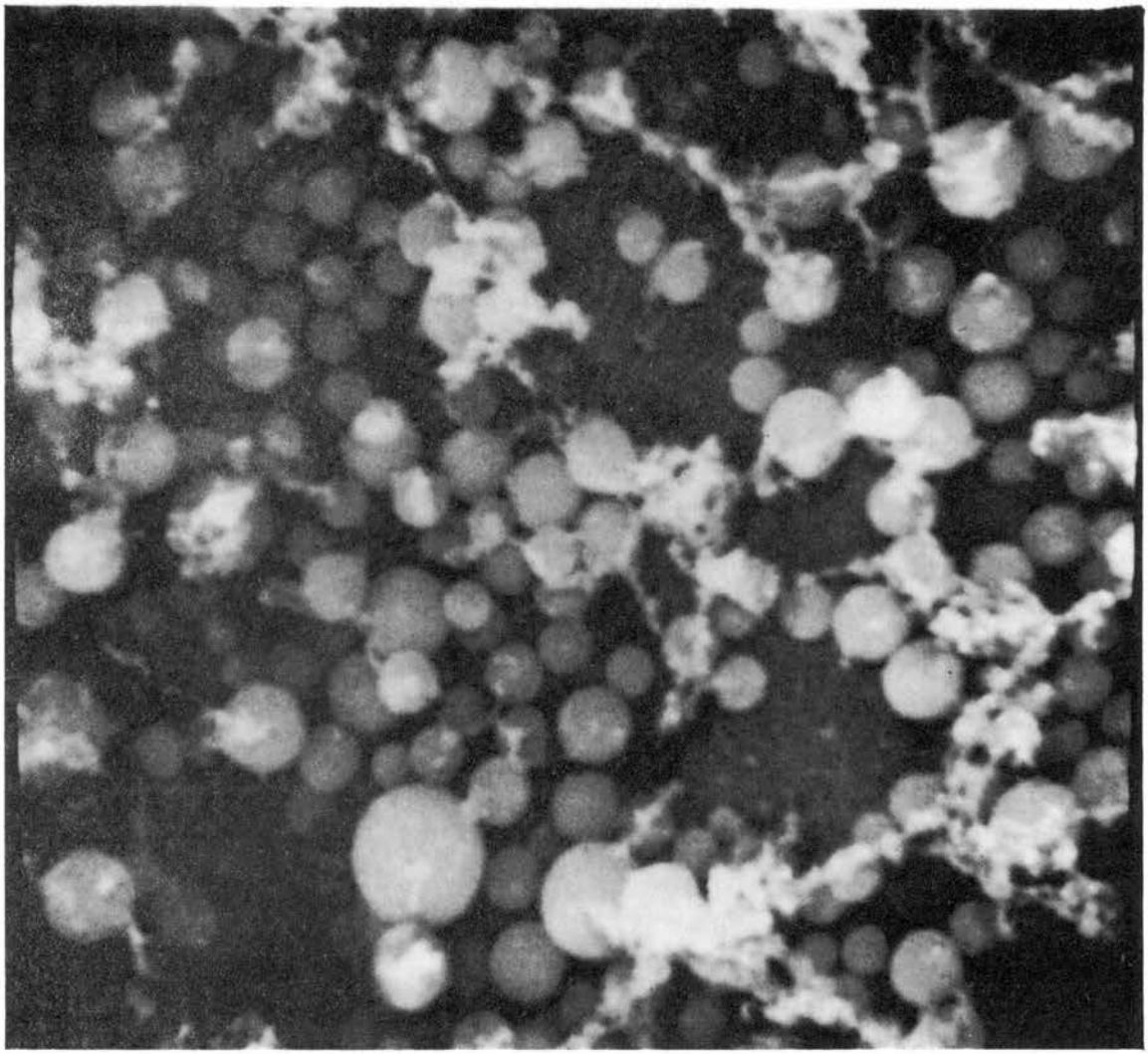

Figure 7. Electron Micrograph of Iron Oxide Aerosol

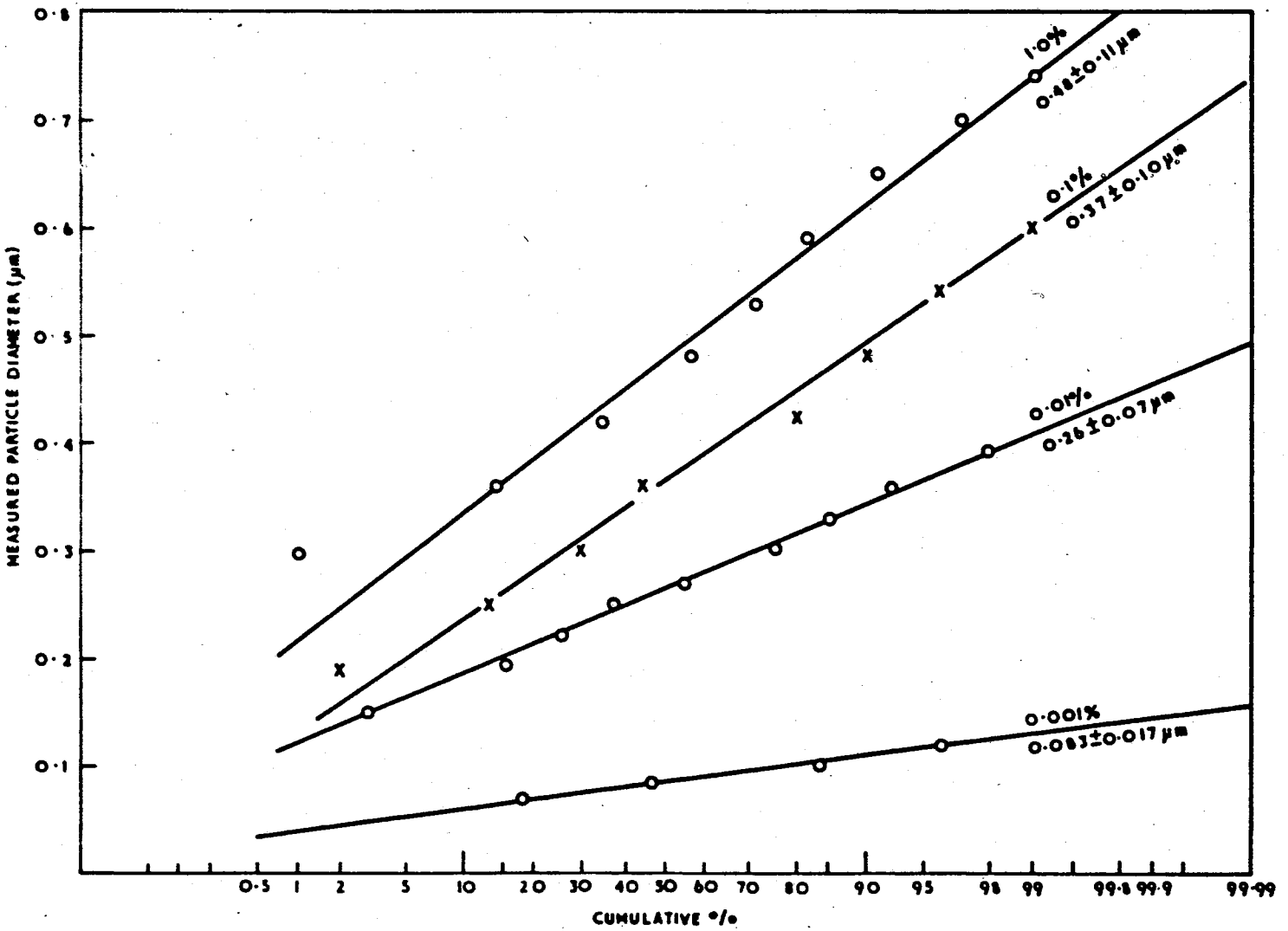

Figure 8. Particle Size Distributions for Different Sol Concentrations

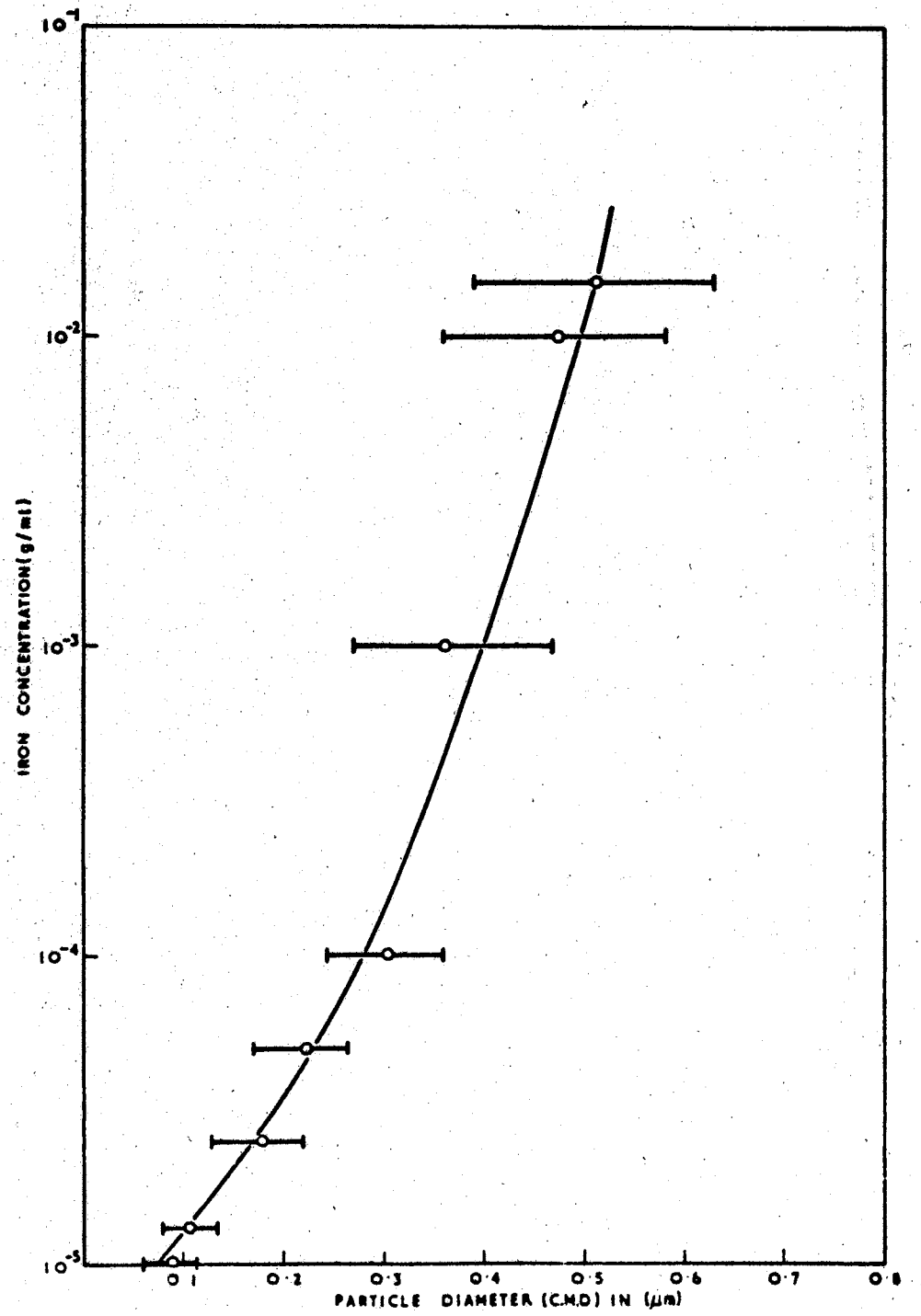

Figure 9. Particle Diameter vs. Sol Concentration

produced by the nebulizer, the diameter should vary linearly with the cube root of the iron concentration. Because the rapid drying technique used gives hollow particles, the relevant diameter to use would be the aerodynamic diameter (AMD). Conversion from CMD to AMD requires knowledge of the particle density. Again because of the hollow nature of the particles, the particle density (iron oxide) will be less than the bulk density or iron oxide.

The iron oxide density of the particles was derived from the measured volume distribution of the particles (electron micrographs) and the known mass of iron oxide in the original 3 μm sol droplet. The results are plotted on Figure 10 showing that the observed density approaches the bulk density (3.5) at particle sizes greater than 0.55 μm but drops rapidly with particle size showing a minimum (and sudden change in density gradient) at a particle diameter of 0.3 μm. This relationship was checked by determining particle iron oxide denisty by an alternative technique. The sol was now manufactured from Fe-59 labelled ferric chloride solution and the radioactive label used as a tag to determine iron oxide mass in a known volume of aerosol particles. The number of aerosol particles in this volume was determined by a calibrated Pollak Counter (29). The Pollak Counter determines particle number density by using the particles as condensation nuclei and measuring the light extinction resulting from the fog produced by adiabatic expansion of the sample volume in a saturated environment. The results of these density measurements are also plotted on Figure 10 and produce excellent agreement with the densities obtained by the first method.

Using the known density-CMD relationship, the aerodynamic diameters can be calculated and the data replotted as AMD against the cube root

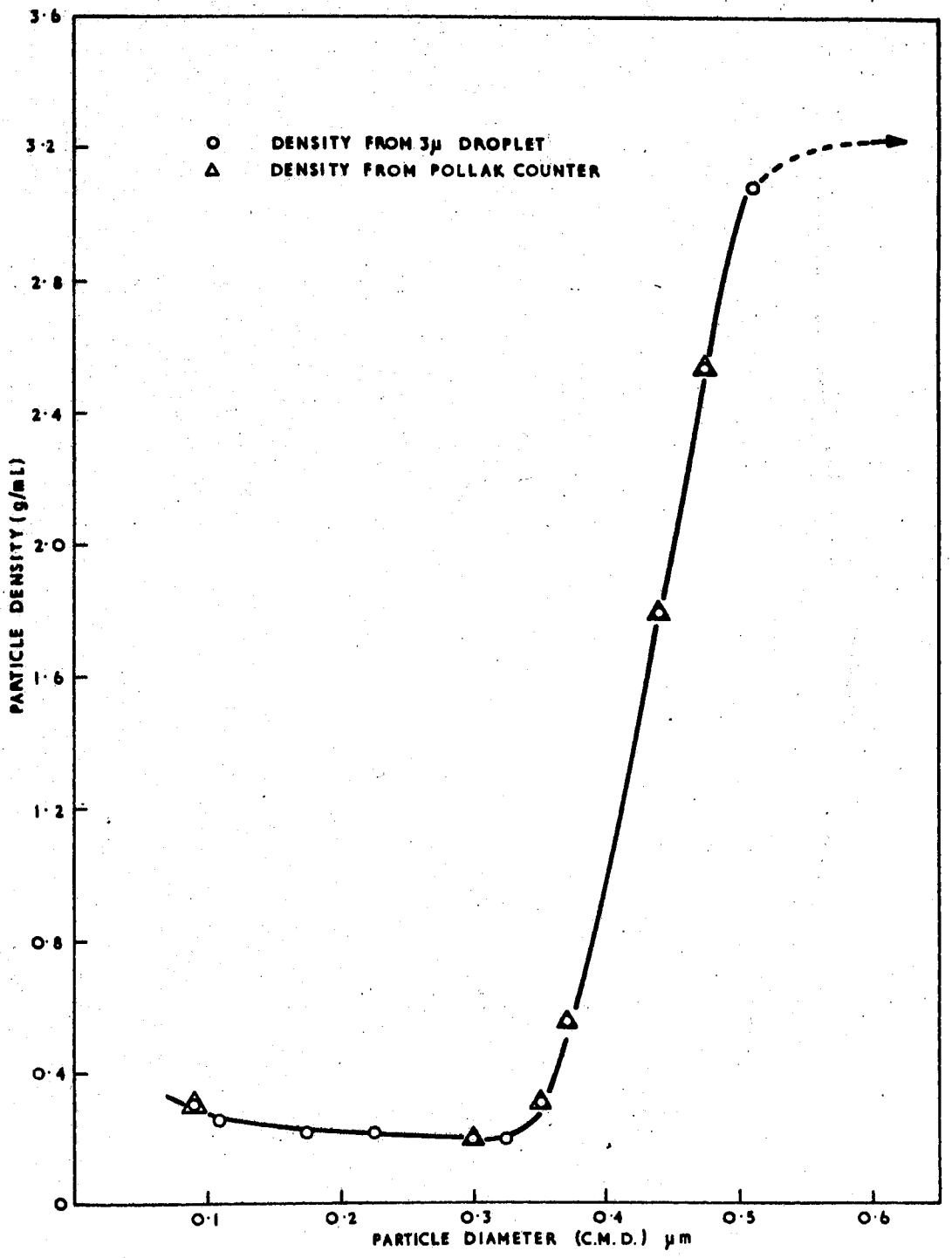

Figure 10. Particle Densities vs. Particle Diameter

of iron concentration (Figure 11). A weighted least-squares-best-fit line is drawn. The intercept at zero diameter is not at zero concentration, with a basic sol particle size (micelle) of the order of 0.01 μm the minimum aerosol particle size obtainable by this method is of this order, corresponding to a concentration of $\simeq 1.3 \times 10^{-4}$ g/l (i.e. $C^{-3} = 5 \times 10^{-2}$)(27).

Discussion

The idea that the ferric oxide aerosol particles are hollow has been advanced (30). It is known that producing particles from atomizing solutions in volatile solvents may produce a spherical shell if the drying is rapid, and the remainder of the solvent is lost by evaporation after diffusion through the shell. Any explanation of hollow aerosol composition and density must depend on the physical size of the primary sol particle, the micelle, a spherical unit of about 0.01 μm diameter and of density 3.5.

The nebulized droplet, mean size 3 μm, will contain a number of micelles, the mean number being determined solely by the gross iron concentration of the sol. On evaporation of the water, the droplet reduces in size, the final size being determined by the geometry of packing of the micelle units in the sphere.

The extension of this idea semi-empirically explains the shape of the density curve obtained experimentally. Several calculations can be initially made to formulate a shell model of the aerosol. If the unit micelle has a diameter 0.01 μm, the number of micelles necessary to satisfy the mass requirements of each particle size A and the maximum number of micelles which can be accommodated in each spherical shell of

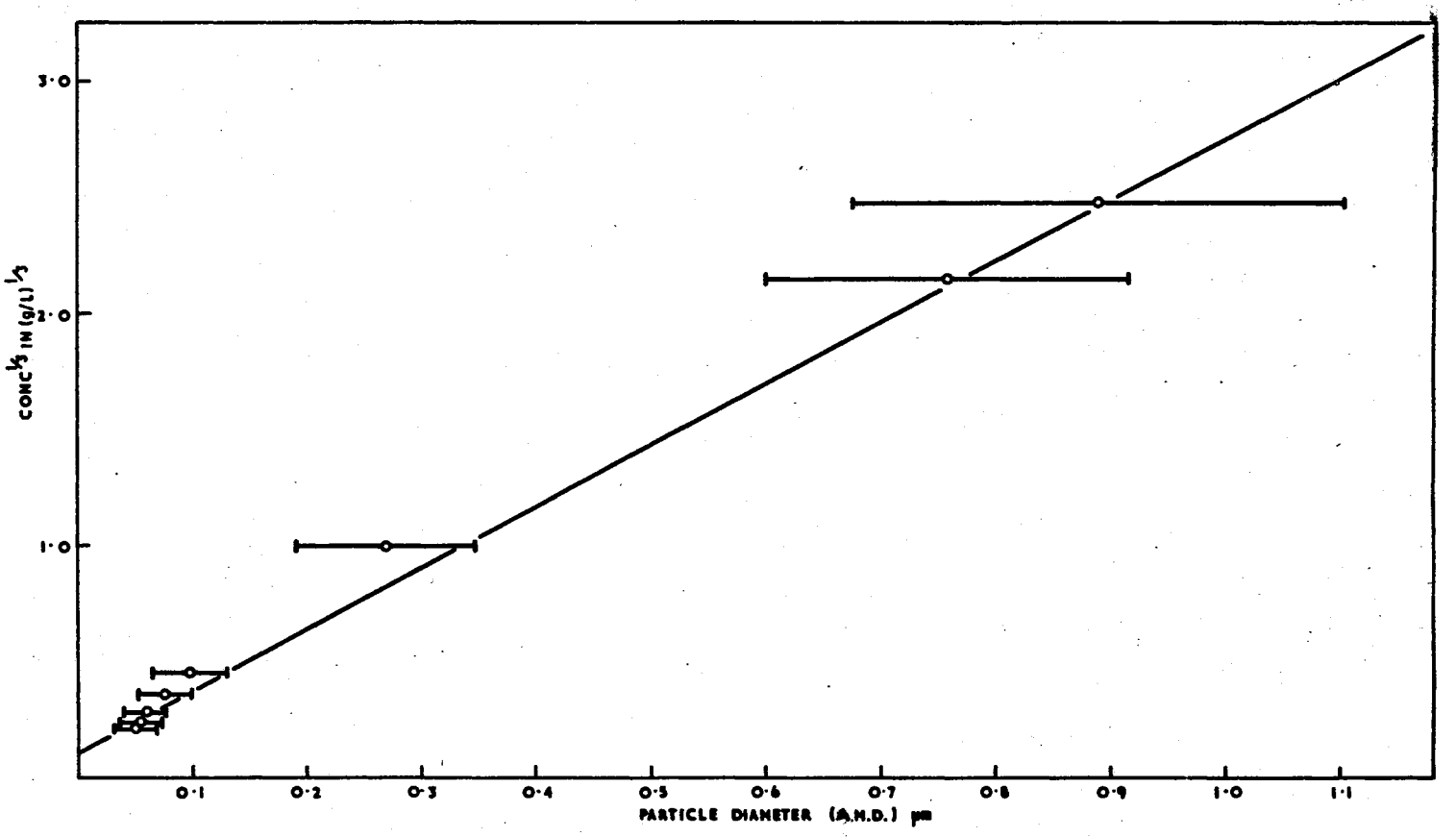

Figure 11. Particle Aerodynamic Diameter vs. Sol Concentration

defined diameter can be calculated. Then the minimum number of shells required to accomodate the required number of micelles per particle can be determined.

Table I lists a few typical figures from such an argument using 0.01 μm micelles. The total number required varies from 78 for a 0.1 μm particle to 1.2×10^5 for a 0.51 μm particle.

The geometry of packing of the micelles in each shell unit is not known. Initially, packing determined by available surface area in each shell and the mean cross sectional area of a micelle was assumed. The maximum number per shell varies from 400 micelles in a shell of diameter 0.1 μm to 10^4 micelles in a shell of diameter 0.5 μm.

Three regions can be studied:

1. Below 0.36 μm diameter--single shell structure
2. Above 0.51 μm diameter--multishell structure--all shells filled.
3. 0.36 μm to 0.51 μm diameter--multishell structure--some empty shells.

Consider a hollow spherical aerosol particle of internal radius R_1 and external radius R_o made up of basic spherical micelled units of diameter D and bulk density p (the density of iron oxide) of 3.5.

The mean density of the aerosol particle is then

$$\overline{p} = \frac{pF \int_{R_1}^{R_o} r^2 \, dr}{\int_{0}^{R_o} r^2 \, dr}$$ where F is a packing fraction constant (<1)

Consider the three regions quoted above:

Region 1. Single shell structure $R_o - R_1 = D$

$$\overline{p} = pF \left[1-(1- \frac{D}{R_o})^3\right] \approx \frac{3pFD}{R_o} \qquad (a)$$

TABLE I

TYPICAL VALUES OF PARAMETERS USED FOR "SHELL" MODEL
--BASIC MICELLE SIZE 0.01 MICRON

Shell Dia. (μ)	Shell No. N	Shell surface area (μm^2)	Available locations per shell A	Total locations required	$\sum_N^i A$	i	No. of shells occupied	Fraction of shells occupied q
0.10	10	31.4×10^{-3}	4.00×10^{2}	7.80×10^{1}	4.00×10^{2}	10	< 1	0.20
0.11	11	38.0×10^{-3}	4.84×10^{2}	1.00×10^{2}	4.84×10^{2}	11	< 1	0.16
0.18	18	10.2×10^{-2}	1.30×10^{3}	1.98×10^{2}	1.30×10^{3}	18	< 1	0.11
0.23	23	16.6×10^{-2}	2.12×10^{3}	3.90×10^{2}	2.12×10^{3}	23	< 1	0.08
0.31	31	30.2×10^{-2}	3.84×10^{3}	7.80×10^{2}	3.84×10^{3}	31	< 1	0.06
0.35	35	38.5×10^{-2}	4.90×10^{3}	3.90×10^{3}	4.90×10^{3}	35	< 1	0.05
0.37	37	43.0×10^{-2}	5.48×10^{3}	7.80×10^{3}	9.57×10^{3}	35	2	0.10
0.44	44	60.8×10^{-2}	7.74×10^{3}	3.90×10^{4}	4.09×10^{4}	32	7	0.32
0.48	48	72.4×10^{-2}	9.22×10^{3}	7.80×10^{4}	7.82×10^{4}	8	21	0.88

Region 2. All shells full $R_1 = o$

$$\overline{p} = pF \text{ (definition of packing constant F)} \qquad (b)$$

Region 3. Some empty shells [If q is fraction of shells filled, i.e., $q = (R_o - R_1)/R_o$]

$$\overline{p} = pF\,[1-(1-q)^3] \qquad (c)$$

From experimental observations, equation (a), Region 1 applied at $R_o \leq 0.18$ and $\overline{p} = 0.2$, i.e., FD = 0.00342 μm.

The observed maximum density in Region 2 is 3.2 and has also been observed by other workers (4). This gives a value of packing fraction, F, as 0.91 and the micelle diameter D, as 0.0038 μm.

A comparative plot of "theoretical" density and the experimental density cannot be made without assuming values for q in equation (c). Using a basic micelle diameter of 0.004 μm, Tabel II gives some values of derived values of q. Figure 12 then plots the comparisons between observed density (experimental points and the smooth curve derived from the above shell model). At particle diameters below 0.2 μm the experimental densities lie below the curve. This discrepancy arises from ignoring the higher order terms in equation (a).

This work does not disagree with the mean densities of iron oxide aerosol particles observed by other workers. The published data has been with particle diameters greater than 0.5 μm when a mean density of 3.2 is obtained.

Experimental data on the leaching of radioactive label from particles both <u>in vitro</u> and <u>in vivo</u> agree well with the above theory that leaching is a function of the exposed surface area of micelles. The degree of leaching observed experimentally varies with particle size

TABLE II

TYPICAL VALUES OF PARAMETERS USED FOR "SHELL" MODEL
--BASIC MICELLE SIZE 0.004 MICRON

Shell Dia. (μ)	Shell No. N	Shell surface area (μm^2)	Available locations per shell A	Total locations required	$\sum_{N}^{i} A$	i	No. of shells occupied	Fraction of shells occupied q
0.094	23	27.9×10^{-3}	2.12×10^{3}	1.13×10^{3}	2.12×10^{3}	23	1	0.083
0.111	27	38.5×10^{-3}	2.92×10^{3}	1.43×10^{3}	2.92×10^{3}	27	1	0.072
0.180	44	10.2×10^{-2}	7.75×10^{3}	2.86×10^{3}	7.75×10^{3}	44	1	0.045
0.226	55	16.0×10^{-2}	1.21×10^{4}	5.64×10^{3}	1.21×10^{4}	55	1	0.036
0.312	76	30.5×10^{-2}	2.31×10^{4}	1.13×10^{4}	2.25×10^{4}	76	1	0.026
0.349	85	38.2×10^{-2}	2.89×10^{4}	5.64×10^{4}	5.65×10^{4}	83	2	0.047
0.365	89	41.8×10^{-2}	3.17×10^{4}	1.13×10^{5}	1.18×10^{5}	83	4	0.089
0.439	107	60.5×10^{-2}	4.58×10^{4}	5.64×10^{5}	5.69×10^{5}	75	17	0.31
0.476	116	71.1×10^{-2}	5.38×10^{4}	1.13×10^{6}	1.13×10^{6}	4	57	0.98

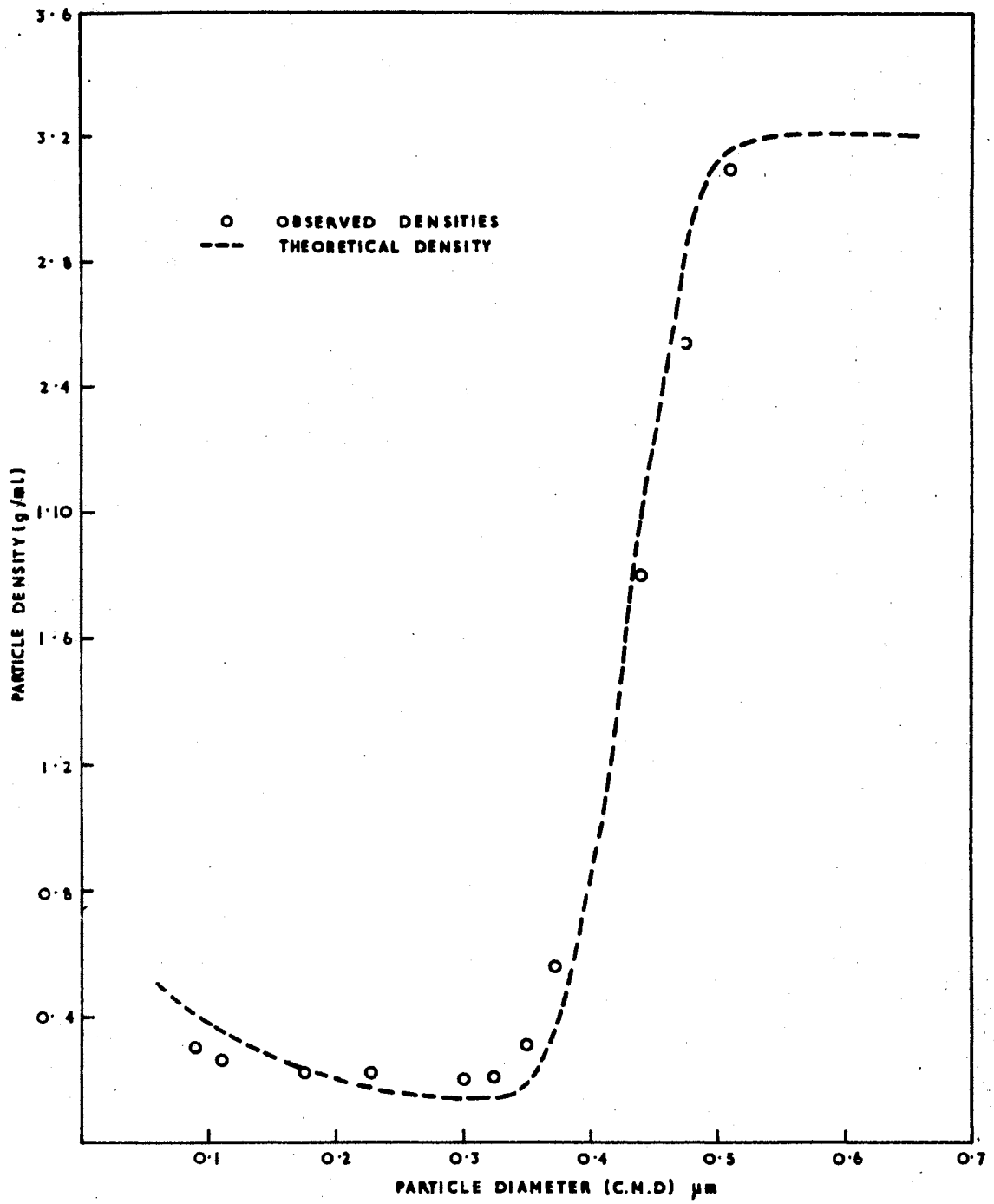

Figure 12. Theoretical Particle Density vs. Particle Diameter

when all other variables are kept constant. For example the relative leaching of Cr-51 from the particles is 1.2% at 0.51 μm and 14% at 0.1 μm. This ratio is 0.086. The ratio of total micelle units to micelle units in the outer shell is 11.25 for the 0.51 μm particle and 1.0 for the 0.1 μm particle, giving a relative available surface area ratio of 0.089 which agrees very well with the observed leaching characteristics.

CHAPTER V

THE INHALATION OF INSOLUBLE IRON OXIDE PARTICLES IN THE SUB-MICRON RANGE PART I-- CHROMIUM-51 LABELLED AEROSOLS

The previous chapter reported on the performance of a high efficiency aerosol generation apparatus to produce insoluble ferric oxide particles in the size range 0.1 μm to 0.5 μm CMD (31). That chapter reported on the overall efficiency of the equipment, the size range distribution of the particles, and gave a simple semi-empirical theory of the mechanism of particle formation to explain the observed density-size relationship.

In this chapter inhalation of Cr-51 labelled aerosols by volunteer subjects, lung retention of the particles, magnitudes and modes of excretion from the body and the resistance of the radioactive label to leaching both *in vivo* and *in vitro* will be discussed.

Chromium-51 was chosen as the radioactive label for the first series of inhalation studies because of the low absorbed dose to the lungs of the volunteers (less than 20 mrem), the simplicity of detection of its single 320 KeV gamma line *in vivo*, and its convenient half period of 27 days. The extension of these inhalation studies to Pu-237 provides valuable information regarding the detection and estimation of more hazardous materials in the human lung (e.g., Pu-239 and U-235). Prior to such work it was necessary to have a good under-

standing of the behavior of the ferric oxide particles in the lungs following an inhalation. This information is provided by the Cr-51 experiments both by in vivo detection and by excretion analysis.

This work does not attempt to simulate any specific aerosol encountered in any specific operational health physics area, nor does it make any attempt to use normal breathing patterns. Both particle size and breathing pattern were selected so as to give a maximum retained fraction in the lung, i.e., to maximum pulmonary deposition rather than deposition in the upper respiratory tract or the nasopharynx.

Preparation and Labelling of the Sol

Deionization levels of better than 90% were achieved by the use of semi-permeable membranes with both ferric chloride and ferric nitrate solutions. The final pH values of the sol were in the range 3.5 to 4.5. The stability of the sol and the efficiency of labelling both depend critically on the pH value. Labelling is relatively simple with sols of high iron concentrations (2% iron by weight) and large sol volumes (10 ml) but the limited availability of some of the other tagging isotopes (Pu-237) meant that it was desirable that all the available isotope was tagged to a sol whose parameters were those required for the inhalation, i.e., a sol of volume 0.2 ml and of iron concentration 0.001% by weight. Although such restrictions were not necessary for the Cr-51 labelling, plenty of Cr-51 activity being available, the more restrictive techniques were developed and tested using this isotope. Carrier free Cr-51 calibrated solutions were adjusted in pH, taken down to dryness, washed to remove excess acid, and the small volume of sol added to controlled pH. Contact times of around two hours were

sufficient to get labelling efficiencies of the order of 80%. A range of labelled sols were also prepared for the *in vitro* leaching studies.

Two types of Cr-51 labelled iron oxide sol were used for the inhalations. The first consisted of using the chromium in the form of a chromate normally readily soluble; this was termed as "leachable" chromium. The second sol was labelled with chromic chromium after reduction of the chromate with sulphur dioxide. This second sol was termed as "non-leachable" chromium.

The Inhalations

The same subject was used for both sets of inhalations in order to keep the biological variations to a minimum. Similarly, the same breathing pattern was used for both experiments. This pattern consisted of one deep breath of four liters which collapsed the reservoir bag. This breath was held for a period of 18-20 seconds and slowly released back into the bag. The reservoir was finally evacuated through Millepore filters. According to Brown (32) such a breathing technique should ensure maximum short-term retention in the lung ($\sim$100%). The location of deposition and long-term retention pattern is a function of particle size (8). To give maximum deposition in the pulmonary region of the respiratory tract, the particle size of 0.05 (AMD) was chosen.

In Vivo Detection

All measurements were done on the Winfrith Whole Body Monitor (15). Lung burdens were determined with one of 5 in. x 4 in. NaI (Tl) crystals positioned beneath the chest. This crystal was calibrated using a realistic chest phantom developed for Pu-239 *in vivo* detection (18).

Total body Cr-51 was determined by using a four-crystal array of static 5 in. x 4 in. crystals in a calibrated geometry.

Crude location scans along the chest were done with a 3 in. x 5 in. crystal and a focused slit collimator (nine slits) of focal length 14 cm. These scans were done manually at three-inch intervals along the chest at various distances from the chest surface.

All counts were of 40 minutes duration, with the scan counts being of four minutes duration per position. The data was stored on punched paper tape for computer analysis. Prior to inhalation the subject's normal body gamma spectrum was recorded.

Bioassay

Both fecal and urine analyses were performed. Total collection of samples was achieved for the first four days after inhalation. The sampling period was gradually extended over a total period of ten weeks. The untreated urine samples were counted on a calibrated scintillation detector for Cr-51 activity while the fecal samples were wet-ashed and reduced to a standard volume prior to scintillation counting.

Results

The same volunteer was used for both inhalations, the time lapse between inhalations being four months. The particle size and breathing pattern was the same for both the "leachable" chromium inhalation and the "non-leachable" chromium inhalation. The results are presented as comparing and contrasting the two types of labelled aerosol inhalations. All retention and excretion curves were analyzed by the method of least squares to give a best-fit to a sum of a series of exponential terms

and are presented graphically after correction for radioactive decay.

Figure 13 shows the lung retention curves and are expressed as a percentage of the initital activity inhaled ($\sim 1\,\mu Ci$). Both curves show a long-term retention component with a half period of 270 ± 20 days. In the case of the "non-leachable" chromium this term predominates and has a magnitude of 82% of the initially inhaled material (showing that the aims of obtaining a maximum deposition of long-term retained aerosol had been achieved). The magnitude of the long-term component in the case of the "leachable" chromium was 38%. Both curves show a short-term component representing the physical transfer of material from the naso-pharynx and upper respiratory tract into the gut. These half periods of 0.3 and 0.6 days can be considered identical considering the errors in analysis at short time periods and the paucity of experimental data during the first day. This early clearance period has been studied fully by other workers(22). The magnitudes of this early clearance phase are very comparable at 21% (leachable) and 18% (non-leachable) showing that the breathing pattern and particle size were well matched in the two experiments. The "leachable" chromium also exhibited a third exponential term of half period 3 ± 1 days and magnitude 41%. This term is absent in the "non-leachable" material and represents the leaching of the chromium label from the retained iron oxide particles and transfer of the soluble chromate ion into the blood stream where it is complexed and excreted via the kidneys.

The whole body retention curves are not shown here but are very similar to those of the lung, showing long-term retention components of 300 ± 30 days and short-term clearances of 0.5 day half life. The third component in the "leachable" chromium inhalation had a half period

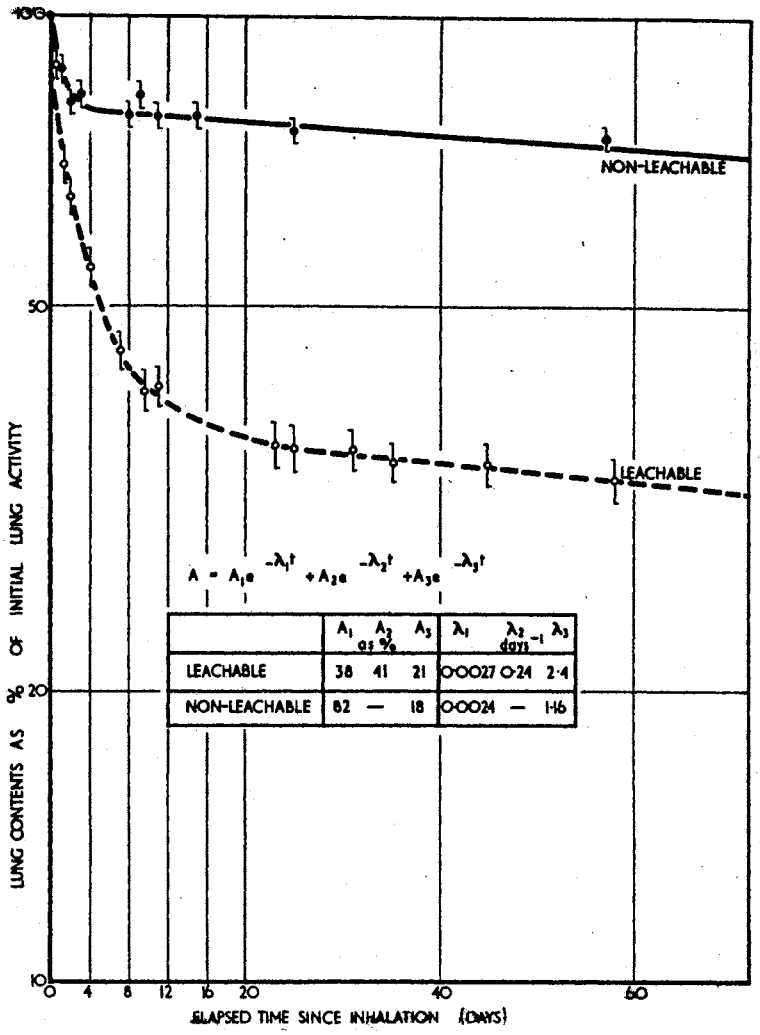

Figure 13. Lung Retention of Cr-51 Labelled Particles

of 6 ± 1.5 days. The magnitudes of all these components, expressed as percentages, are very similar to those reported for the lung contents, and the whole body activity is initially some 20% higher than the lung activity.

The lung retention curves can be compared directly with the fecal excretion curves (Figure 14) and the urinary excretion curves (Figure 15). Both sets of excretion curves show a rapid clearance phase with half periods in the range 0.4 to 0.7 days. Again the errors in analysis and paucity of early samples are such that no significance can be given to differences in these half periods. The magnitude of the early fecal clearance is roughly the same in both inhalations, peak clearance being observed at day 2 at approximately 25% of the inhaled material. These findings agree with the early lung clearance of 20% in the first day, the material being transferred to the gut and eventually excreted in feces.

The urinary clearances differ by a factor of 10 between the two inhalations (Figure 15). The "non-leachable" chromium shows low urinary detection to 0.04% per day. The "leachable" chromium shows a high early clearance component of 20% per day on day 1 and accounts for the "leached" chromium label seen in the lung retention curve.

A longer term exponential is also seen in the fecal excretion of "non-leachable" material with a half period of 240 days and a magnitude of 0.1% per day of the initial lung activity. Although this long-term component is not seen in the fecal excretion of "leachable" material, the excretion levels after day 8 are below the limits of detection of 0.04% per day, and as such no analysis of this term was attempted.

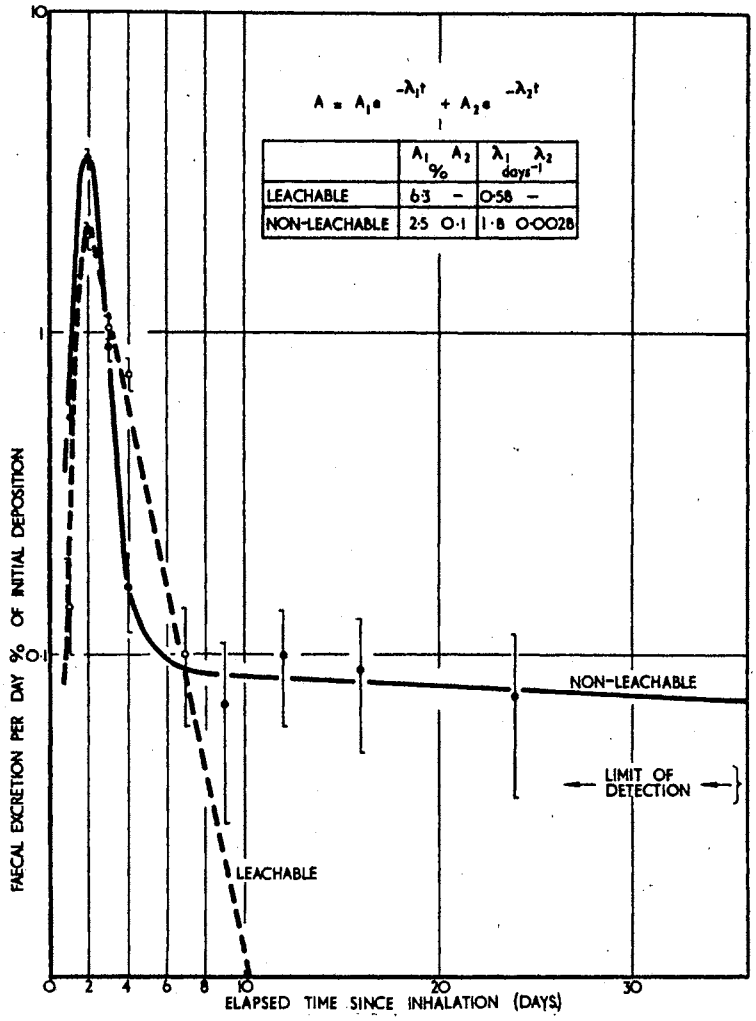

Figure 14. Fecal Clearance of Cr-51 Labelled Particles

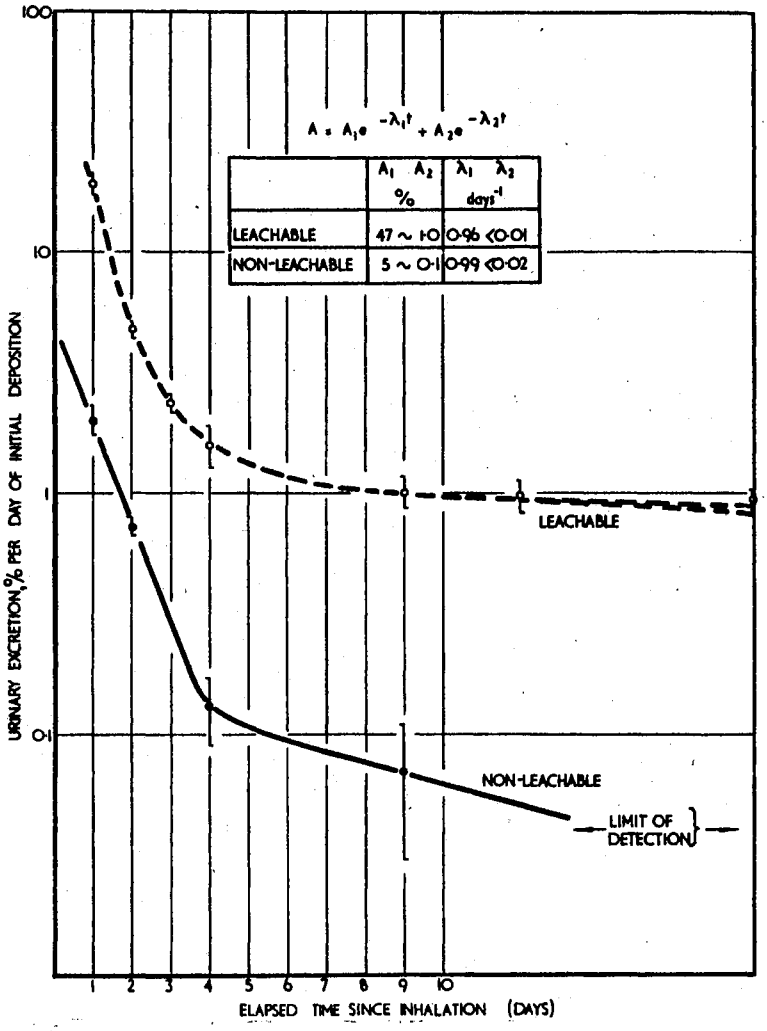

Figure 15. Urinary Clearance of Cr-51 Labelled Particles

Both urine excretion curves show evidence of a long-term component, but again excretion levels are very close to the limits of detection, and no accurate assessments could be made. Approximately 1% of the initial intake is excreted per day as long-term urinary excretion of "leachable" chromium with a half period in excess of 100 days. The "non-leachable" long-term excretion is again a factor of 10 (0.1% per day) down on the "leachable" material.

These results are discussed more fully later in the chapter and compared with the results obtained from in vitro leaching, but overall agreement in excretion patterns and retained fractions can be seen. This agreement can be expressed graphically by plotting the integrated excretion against time and comparing this to the drop in lung counts (Figure 16). In both cases accountability of better than 80% is achieved.

The activities inhaled ($\sim$1 μCi) were not sufficient to enable accurate scans to be done over the chest region to obtain detailed information of the sites of deposition of the ferric oxide particles. The results from the manual scans using the collimated crystal over the chest are presented in Figure 17. Note the early clearance of the upper lung, the predominant deposition in the deep lung, and the increase in counts at the base of the lungs on days 2 and 3 as material passes down the esophagus to the gastrointestinal (GI) tract.

The overall picture of deposition in deep lung agrees well with observed high long-term retention in the lung (pulmonary deposition) and demonstrates the success of choice of particle size and breathing pattern. Comparison between the two inhalations shows that deposition was a little higher in the lung with the "non-leachable" inhalation.

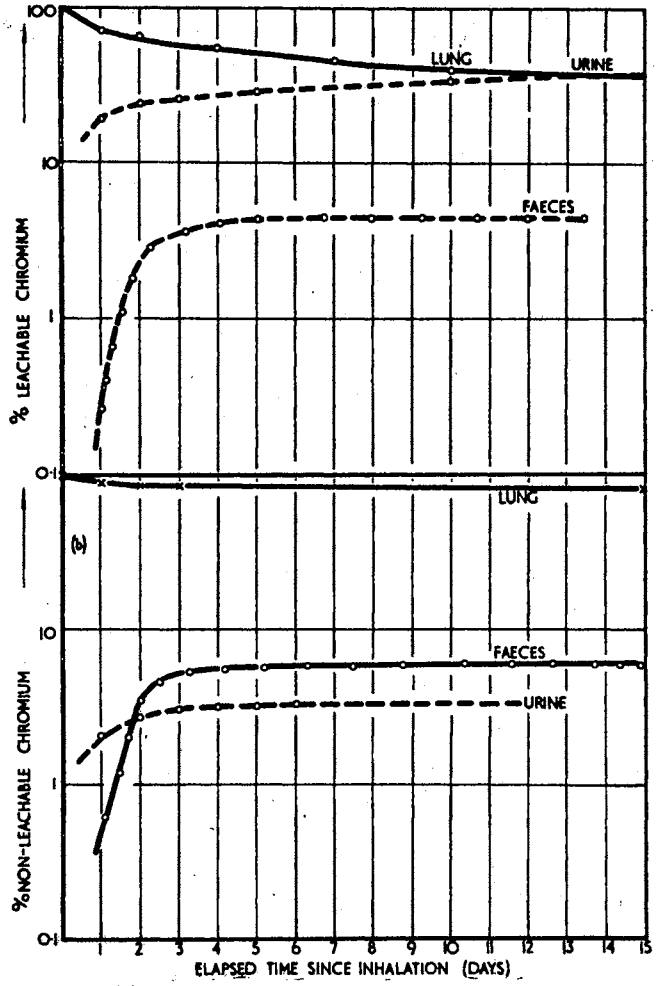

Figure 16. Cumulative Excretion and Retention Fractions

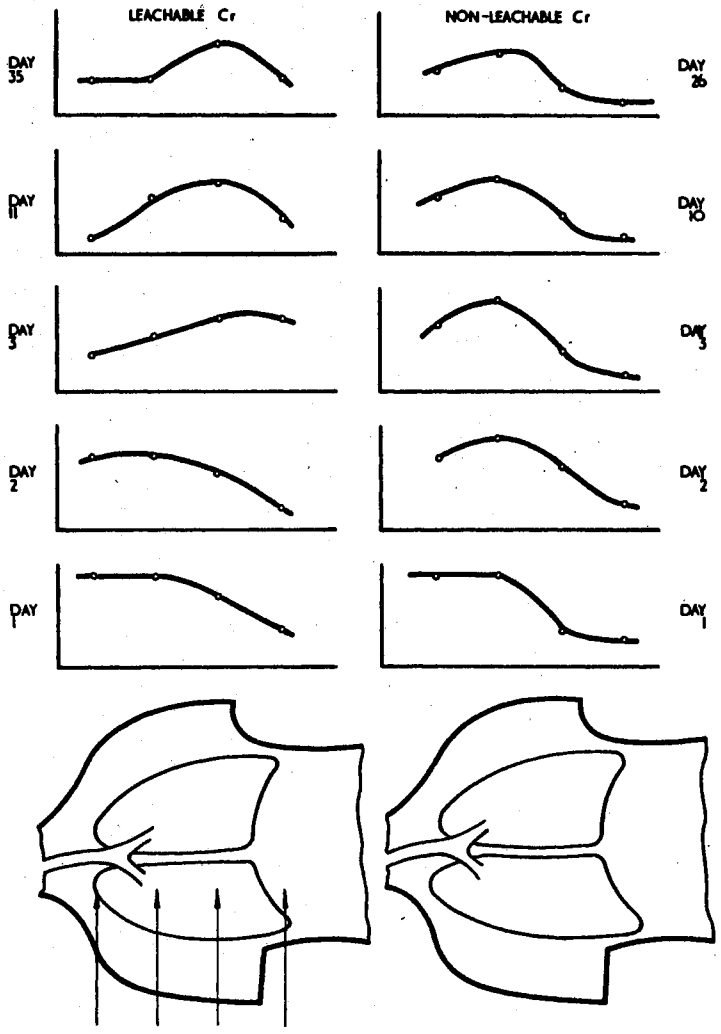

Figure 17. Distribution of Cr-51 Activity in Lungs

but the basic deposition patterns are very similar. The activity scales on Figure 17 are normalized to give equal deposition in the upper respiratory tract on day 1.

The relevant experiments for these chromium inhalations consisted of a suspension of tagged aerosol particles (0.05 μm AMD) in isotonic saline solution. Two approaches were tried. Small samples were taken from a large-volume, closed system and analysed for chromium in the liquid (filtrate) phase and compared to retained chromium levels on the iron oxide. The second approach was to completely remove all chromate ions from the system via a semi-permeable membrane as they leached off the suspension of ferric oxide particles. This second system is not in equilibrium and is more typical of the situation as it occurs in the lung. The results from these experiments are presented graphically in Figure 18.

Only two curves are shown in this figure: the first curve shows "non-leachable" material in a large-volume, closed system, giving a half period of leaching of 3.4 days and a maximum availability for leaching of 9%; the second curve shows "leachable" chromium in the semi-permeable membrane system, giving a half period of leaching of 2.6 days and a maximum availability for leaching of 63%. Similar results were obtained for the other two conditions.

Dose to Volunteer

The amount of activity inhaled in each of the experiments was 1 μCi Cr-51 (± 10%). Calculations utilizing observed lung retention patterns and using 1000 g as the mass of the lungs yield the following

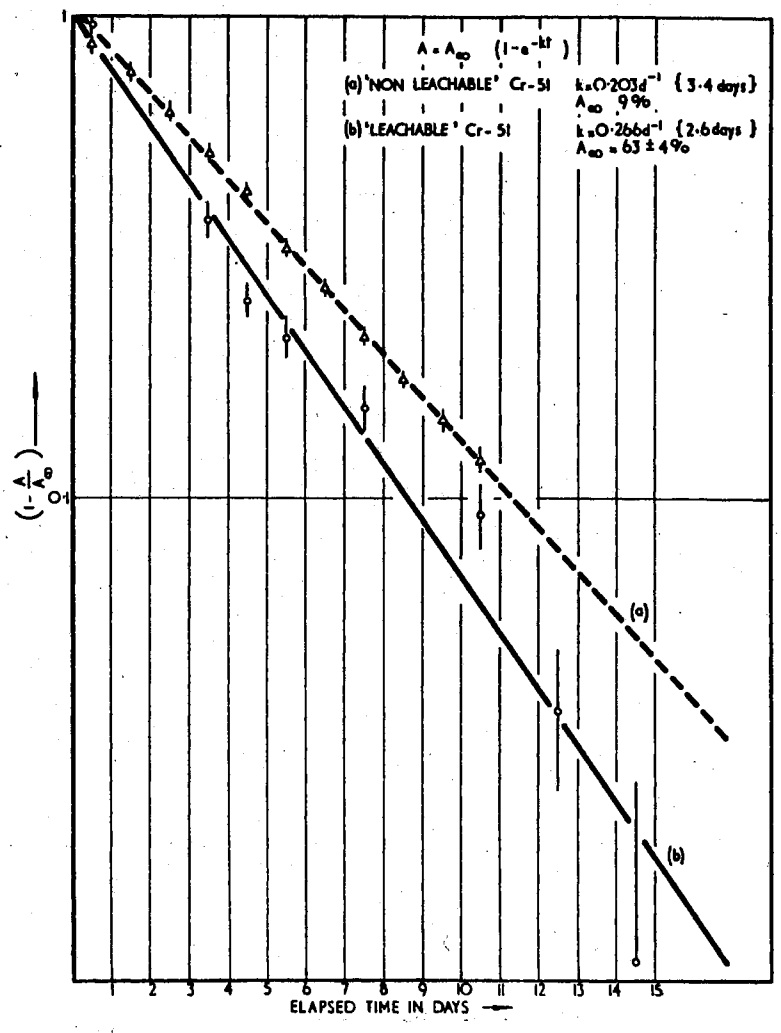

Figure 18. Leaching of Cr-51 In Vitro

total absorbed doses to the volunteer's lungs:

Inhalation 1 (leachable chromium)	11 mrem
Inhalation 2 (non-leachable chromium)	21 mrem
Total to volunteer	32 mrem

The recovery via urine and feces indicate that no long-term retention in blood (or liver or spleen) occurred, and the rapid transfer through the GI tract meant that doses to other organs are negligible compared to the lung dose.

Discussion

Viewed in the context of part of a thesis, the primary objectives of the chromium inhalations were to demonstrate that the overall high efficiency of aerosol production achieved by the nebulization apparatus could be maintained throughout the inhalation procedure and could give a high fraction of the particles retained in the lung with a long clearance period (~ 200 days). This high retention is achieved by choice of particle size and breathing pattern. It is this long-term retained fraction that is usually measured by *in vivo* detection techniques for more hazardous isotopes in the lung (e.g., Pu-239 and U-235) and which contributes a high percentage of the absorbed dose to the lung from such isotopes.

The early studies of the iron oxide particles produced, at the sizes required for these inhalations, showed them to be hollow spheres with a large surface area available for the leaching off of the isotopic tag. The density of these particles, 0.1 g/ml, is much less than the density of the larger particles used by other workers; above a diameter of 0.6 μm a constant density of 3.2 g/ml is obtained. Leaching of the

isotopic tag was, therefore, expected, and the chromium inhalation experiments were also aimed at measuring such effects.

The use of the terminology "leachable" and "non-leachable" rather than the more usual terms--soluble (transportable) and insoluble (non-transportable)--emphasize the fact that the phenomenon is one of removal of the isotopic label from the outer surfaces of the insoluble iron oxide particle rather than solubilization of the particle itself. This reasoning is confirmed in the animal experiments where Cr-51 labelled ferric (Fe-59) oxide particles are used and the Cr/Fe ratio studied.

The earlier chapter postulated that the aerosol particles were built up from discrete sol units (micelles) of diameter 0.004 μm and that the relative leaching from particles of different sizes was a function of the surface area of the exposed micelles in the outer shell of the iron oxide particle. Such a postulation was confirmed experimentally. At a particle size 0.1 μm (CMD) the shell model of particle structure would indicate that approximately 54% of the available integrated micelle surface area was available for leaching. The <u>in vitro</u> leaching data can be applied to the <u>in vivo</u> results to quantitatively correct for leached Cr-51 activity.

The <u>in vitro</u> leaching results give a maximum of 63% available Cr-51 from the "leachable" aerosol with a half period of the order of 3 ± 0.5 days. Comparison of this figure with the observed lung retention and urinary excretion patterns for the "leachable" inhalation shows a component of 2.9 days half period and 41% amplitude in the lung retention curve and a component of 47% (but only 0.75 days half period)in the urinary excretion curve. The mean of these two figures (44%) with the

allowance for the 21% of the initial activity which was rapidly cleared by fecal excretion, gives a mean percentage of available chromium in the *in vivo* leaching of 56% which compares well with the figures for *in vitro* leaching (63%) and that derived from the "micelle" model (54%). Applying similar arguments to the small amount of leaching seen with the "non-leachable" material, the *in vitro* result is 9% compared with the *in vivo* result of 6.2% of available chromium.

Such an approach explains the magnitude and period of the early urinary excretion but does not explain the fact that the "leachable" inhalation exhibits a long period urinary excretion term which is not seen in the case of the other inhalation. Assuming that the main long-term clearance is via the cilliated escalator, the gut and fecal excretion, long-term urinary excretion can be explained by postulating that the iron oxide particle, made up of an aggregation of smaller micelle units, becomes unstable in the acid environment of the stomach and any remaining chromium, in chromate form, is leached off at this stage and appears in urine rather than feces. Thus no long-term fecal excretion above the MDA is seen in the "leachable" inhalation and no long-term urinary excretion above the MDA is seen in the "non-leachable" inhalation, but the magnitudes and periods of the long-term urinary excretion for "leachable" material (0.8%/d~ 100 days) is comparable with the long-term fecal excretion of "non-leachable" material (0.1%/d, 240 days).

In both inhalations the lung retention curves can be corrected for the removal of the radioactive label by leaching and expressed in terms of percentage of initial deposition of iron oxide particles. Such corrections can be made by assuming the urinary excretion represents excretion of chromium leached from the particles while in lung; this

would obviously be an overestimate of the effect. The alternative applied here was to correct the activity observed in the lung for the known leaching pattern as measured in vitro. Figure 19 shows the lung retention curves for both inhalations after such corrections based on the in vitro leaching curves shown in Figure 18. Because the inhalations were done on the same volunteer subject with identical particle sizes and, as far as was possible, using identical breathing patterns, the retention of iron oxide particles in the lung should be the same when expressed as percentage of initially deposited aerosol. Figure 19 shows that the corrected lung retention points from the two inhalations are indistinguishable within experimental error and the line drawn is the best fit to both sets of points.

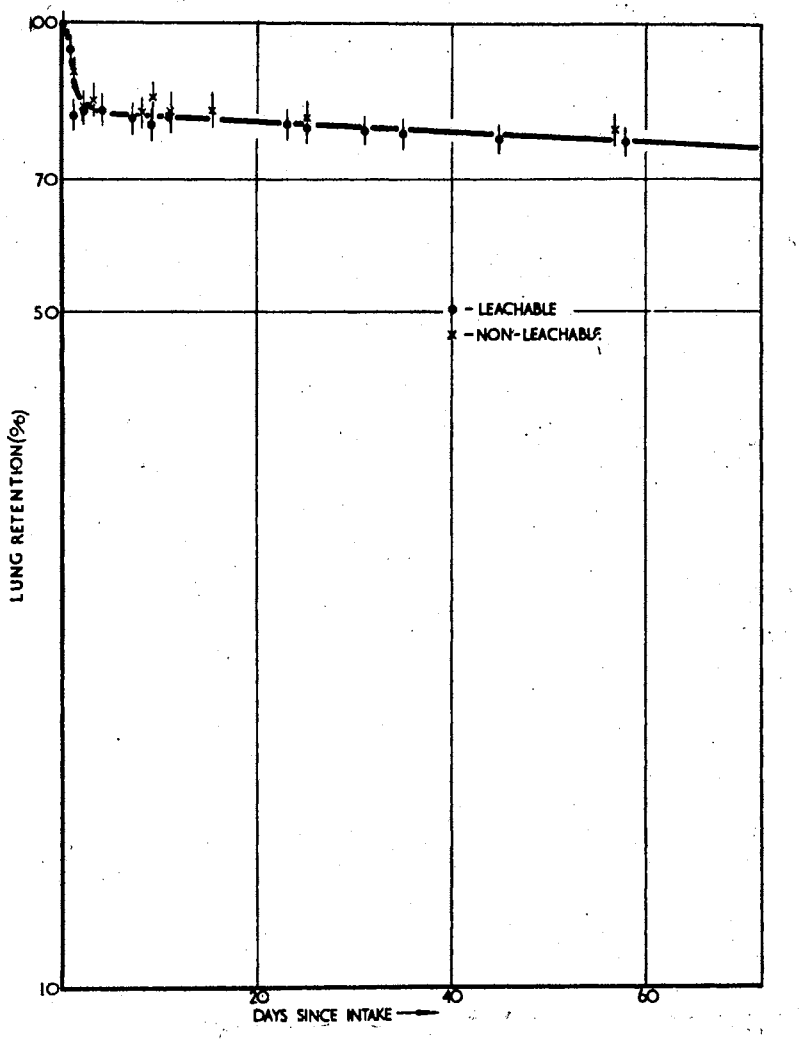

Figure 19. Lung Retention Corrected for Leaching

CHAPTER VI

THE INHALATION OF INSOLUBLE IRON OXIDE PARTICLES IN THE SUB-MICRON RANGE PART II-- PLUTONIUM-237 LABELLED AEROSOLS

The inhalation experiments consisted of two series; one using Cr-51 labelled iron oxide particles was the subject of the previous chapter giving details of the isotopic labelling techniques, the inhalation apparatus, and *in vivo* detection equipment (33). That chapter reported on the studies of lung retention, location of the particles within the thorax region, fecal and urinary excretion, and *in vivo* and *in vitro* leaching studies. It gave a consistent picture of high lung retention ($\sim$ 80%) with a long biological half period ($\sim$ 300 days) in the pulmonary region. The high retention figure was obtained by using small particles (0.05 μm AMD) and an atypical breathing pattern.

This chapter reports on the final series of inhalation studies using aerosols labelled with Pu-237 and attempts to apply the results obtained to the field of the detection of more hazardous materials in the human lung, i.e., Pu-239.

Choice of Plutonium-237

The problems of the detection of Pu-239 in the human lung and the interpretation of the results obtained have been studied in these laboratories and at other centers throughout the world for several

years (34-37). In vivo studies on Pu-239 can only be made after accidental inhalations which are fortunately rare events.

Whereas in the inhalation work reported earlier Cr-51 was picked as the labelling isotope because of the simplicity of its detection in vivo and the low absorbed doses to the lungs of volunteers, Pu-239 was picked because of its close match of low energy decays to Pu-239, i.e., because of the difficulties of its detection in vivo, while maintaining the low absorbed doses to the lung.

Plutonium-239 decays by alpha emission, not detectable by monitoring externally to the body, and by the emission of the L X-rays of uranium in approximately 4% of its disintegrations, the only gamma emissions having abundances of less than 0.01% per alpha. The L X-rays having energies of 13.6, 16.9, and 20.6 KeV can be detected, external to the chest, by means of specially designed low-background gas-filled detectors (34,35). The accuracy of such determinations of Pu-239 in the lung is critically dependent on the location of activity within the chest, i.e., on particle size and breathing pattern, on the subject's body gamma activities, on the subject's body build (obesity), and on the isotopic composition of the plutonium contaminant (17, 38). Basically these difficulties all arise from the facts that the half thickness of the X-rays in soft tissue is small ($\sim$0.6 cm), scattered and degraded gamma radiations in this energy region are very dependent on body build, and the specific X-ray emission of the contaminant can vary by up to a factor of four depending on the irradiation history of the nuclear fuel. Many of these parameters have been studied by using realistic chest phantoms and by measuring the occasional inhalation incident (18, 25).

Any simulator for Pu-239 must have abundant X-ray emissions of the correct energy and be of convenient half life to enable the longer-term retention fractions to be studied (i.e., 10-50 day half period). Naturally the absorbed dose to the lungs of the volunteer must be minimal. The simulator must also have higher energy gamma rays (100-500 KeV) to enable accurate assessment of total lung activity and some location studies to be made by using conventional scintillation detection devices. Most Pu-239 contains a variable amoung of Am-241 which emits a 60 KeV gamma ray. The presence of a low abundance 60 KeV radiation from the simulator is an added advantage.

In practice the choice of isotope satisfying the above requirements is limited, and only two were considered suitable. Protactinium-233 had already been proposed and tested by other workers and Pu-237 had been used in animal work (39, 40). Table III compares the basic data for these two isotopes.

TABLE III

CHOICE OF SIMULATOR FOR PLUTONIUM-239

Isotope	Decay Mode	Half Life (days)	% L X-rays	Gammas		Daughters	Production
				%	KeV		
Pa-233	Beta	27	38	44	310	U-233	Th-232 (n,γ)
Pu-237	E.C.	43	30	40	100	Np-237	U-235 (α,2n)
				(5)	(60)		

Protactinium-233 has the great advantage of being readily available from neutron irradiation of Th-232 while Pu-237 is cyclotron produced. Plutonium-237 was finally chosen because of the presence of the 60 KeV radiations and the low absorbed dose associated with the capture decays.

Production and Preparation of Plutonium-237

Most owners of cyclotrons are understandably very reluctant to have enriched uranium targets in their machines because of the contamination resulting from any target failure. A cyclotron with an external beam facility and high current was needed for the Pu-237 production and the author is very grateful to the Hammersmith Medical Research Center, London, cyclotron unit for supplying irradiation time on their machine. In order to minimize direct production of Pu-236 (α ,3n) and Pu-238 (α ,n) a beam energy of 25.5 MeV was selected and the target, manufactured from highly enriched uranium foil, welded onto an aluminum plate. Table IV summarizes the production details.

TABLE IV

PRODUCTION OF PLUTONIUM-237

REACTION	BEAM ENERGY--25.5 MeV He^4
U-235 (α ,2n) Pu-237	IRRADIATION--80 μA hr
COMPETING REACTIONS	TARGET--0.002"x1"x3" U-235 (93% enriched) foil
U-235 (α ,n) Pu-238 U-235 (α ,3n) Pu-236 U-235 (α ,p2n) U-235 (α ,dn) Np-236 $\xrightarrow[22\ hr]{B}$ Pu-236 U-235 (α ,t) U-235 (α ,p) Np-238 $\xrightarrow[2\ da]{B}$ Pu-238 U-235 (α ,f)	YIELD--4 μCi Pu-237 CHEMISTRY--rapid separation of Np, U, from Pu fraction IMPURITIES--less than 0.03% total alpha (mainly Pu-236)

After the initial chemical separation of the plutonium fraction by a series of ion exchange columns, final purification of the material and activity measurements could procede at a more leisurely pace.

Aerosol Labelling and Production

The aerosol of ferric oxide particles is produced by using an ultrasonic nebulizer to produce monodisperse droplets of a dilute ferric sol which are then dehydrated to the stable iron oxide. Labelling is done in the sol phase. Particle size is previously determined by the iron concentration in the sol phase and particle stability controlled by the production technique of a controlled flow of warm, clean, dry air; a dehydration chamber; and small volumes of sol (0.2 ml). Efficient labelling techniques depend primarily on the pH value of the sol and the chemical form of the isotopic label. Resistance to leaching off of the isotopic label both in vivo and in vitro depends on the chemical form of the label and the particle size.

Because the activity available is limited, the techniques developed required high efficiency of labelling in small volumes (0.2 ml) of dilute sol (0.01% Fe by weight) and an overall high efficiency of aerosol production ($\sim$ 20% from sol to final inhaled fraction). Both these aims were achieved and have been reported elsewhere.

Inhalations

Two volunteers were used for the two inhalations, each breathing in an atypical manner at the extremes of breathing pattern. Neither of the two patterns nor the particle sizes chosen were intended to represent any typical occupational exposure. Subject 1 inhaled an aerosol

of 0.1 μm (CMD) taking a deep breath of four liters and holding for 30 seconds prior to slow exhalation. This technique should ensure maximum deposition in deep lung and was similar to that used in the Cr-51 inhalations (32). Subject 2 inhaled an aerosol of 0.3 μm (CMD) with shallow breathing of 250 mls/breath (minute volume 5 liters) ensuring deposition, if any, in the upper respiratory tract and nasopharyngal (NP) regions. In both cases the exhaled fractions were collected and assayed. About 0.1 μCi Pu-237 was initially retained in the respiratory system for both volunteers.

Measurements

Measurements were taken below the chest with a large-area (5 in. diameter) thin NaI crystal (2 mm thick) which was partially collimated. This crystal viewed both the 60 KeV and 100 KeV peaks. Above the chest one or two gas-filled proportional counters were used to detect the 17 KeV X-radiations. These detectors, specifically designed for the detection of Pu-239 *in vivo*, were used with various gas fillings to give a range of differing efficiencies of detection (41).

Crude location scans were done on the 100 KeV line using a nine slit focused collimator on a 5 in. x 3 in. NaI crystal. The other detectors, mentioned above, were also moved over and under the chest to give a range of responses and further information on the gross deposition of the aerosol in the chest.

Initial calibrations were done with Pu-237 sources in the lungs of a realistic chest phantom which was corrected for the individual body builds of the volunteers (17, 18).

Measurements were taken daily for one week and at intervals up to

seven weeks.

Raw urine was counted in a calibrated geometry using the 100 KeV radiations detected by a shielded 3 in. x 3 in. NaI detector. Fecal samples were wet-ashed and reduced to a standard volume of 50 ml prior to counting on the same detector. The sampling period varied from total collection over the first few days to once per week at later times. Once the activity was below the limits of detection of the crystal, sampling was stopped.

Results

All results were decay corrected back to the time of inhalation and presented as comparing and contrasting the two subjects.

Subject 1

Inhalation pattern	1 breath (4 liters)--hold 30 seconds
Particle size	0.1 μm (CMD)
Weight	82 Kg
Height	178 cm
Activity retained (Day 0)	122 nCi (total respiratory system)

Subject 2

Inhalation pattern	very shallow breathing at 250 ml--total air breathed 10 liters
Particle size	0.3 μm (CMD)
Weight	80 Kg
Height	191 cm
Activity retained (Day 0)	85 nCi (total respiratory system)

The lung contents are shown on Figure 20, as derived from the calibrated thin crystal beneath the chest of the supine subject, all content being expressed as a percentage of the total initial deposit of activity. The two curves demonstrate markedly the effects of change of breathing pattern. Case 1 is very similar to the retention pattern previously reported for the inhalation of Cr-51 labelled particles of

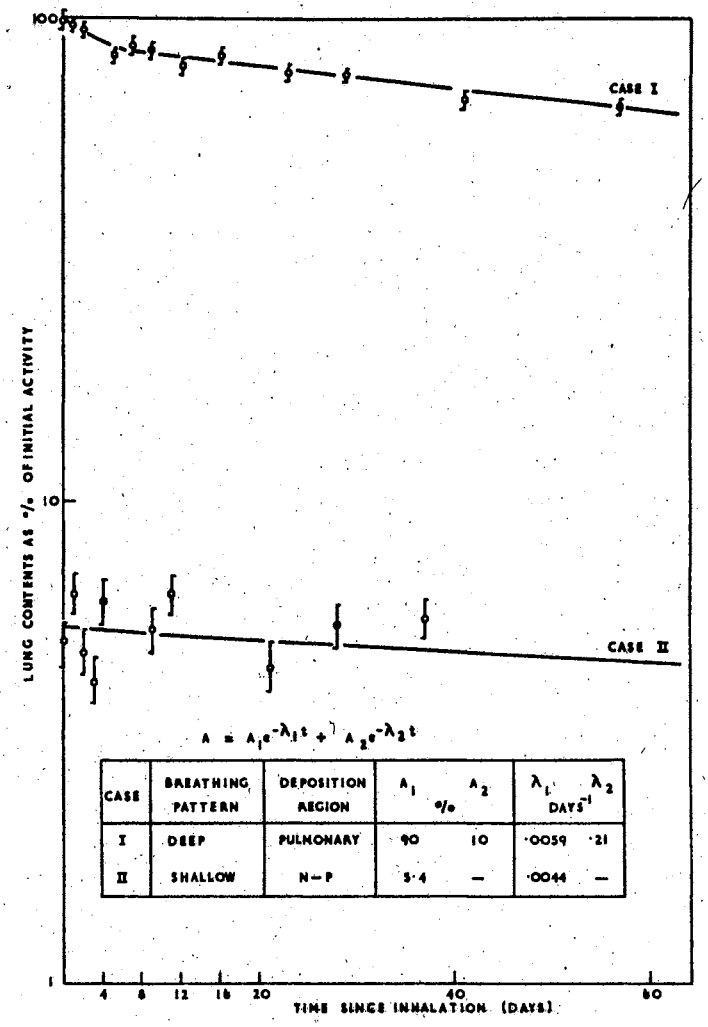

$$A = A_1 e^{-\lambda_1 t} + A_2 e^{-\lambda_2 t}$$

CASE	BREATHING PATTERN	DEPOSITION REGION	A_1 %	A_2 %	λ_1 DAYS^{-1}	λ_2 DAYS^{-1}
I	DEEP	PULMONARY	90	10	·0059	·21
II	SHALLOW	N–P	5·4	—	·0044	—

Figure 20. Lung Retention of Pu-237 Labelled Particles

this size (0.1 μm CMD) with a high retained fraction (90%) of a long half period of clearance (118 days) and a shorter-term clearance of 3.3 days half period representing only 10% of the initial activity. All the initial deposited activity is seen in the trachea-bronchial (T-B) and pulmonary regions viewed by the detector.

In Case 2, when the shallow breathing pattern did not markedly exceed the inert gas deadspace, the maximum initial deposition was not in the field of view of the detector, i.e., in the NP region, and only 5.4% of the initially deposited activity appeared in the T-B/pulmonary regions. The statistics of counting this low percentage is such that the early clearance phase cannot be estimated and a long-term retention half period of 160 days is derived from this component.

Figures 21 and 22 show the fecal and urinary excretion curves respectively. In Case 1, pulmonary deposition, 3.5% of the initial activity is cleared within the first eight days with a clearance period, after the peak of excretion at day 4, of 0.8 days. A long term excretion period of 72 ± 30 days was also present with an amplitude of approximately 0.2% of the activity/day. A single exponential urinary clearance was seen in this case with a half period of 3.6 days and an initial amplitude of 0.19% of the initial activity. This half period of approximately 3.5 days seen both in the urinary excretion and in the lung clearance was also observed in the earlier Cr-51 inhalations. It represents the <u>in vivo</u> leaching of the small soluble plutonium fraction from the surface of the iron oxide aerosol and was studied in an earlier chapter.

In Case 2, deposition in upper respiratory tract and NP region, 95% of the deposited activity was cleared within the first eight days

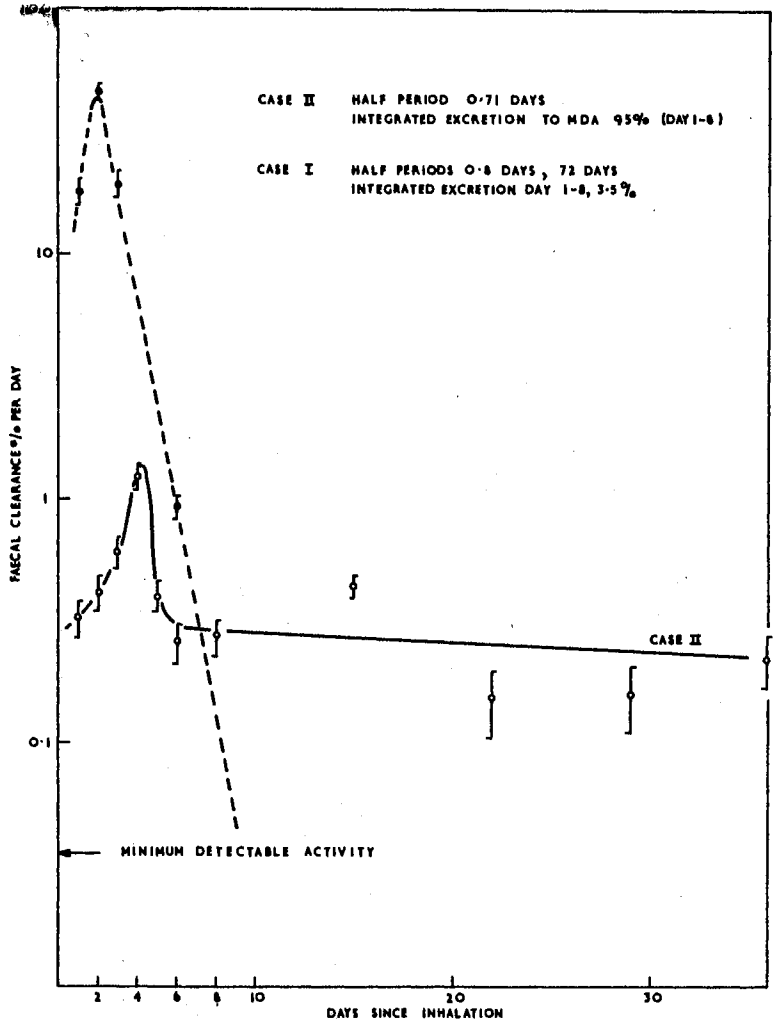

Figure 21. Fecal Clearance of Pu-237 Labelled Particles

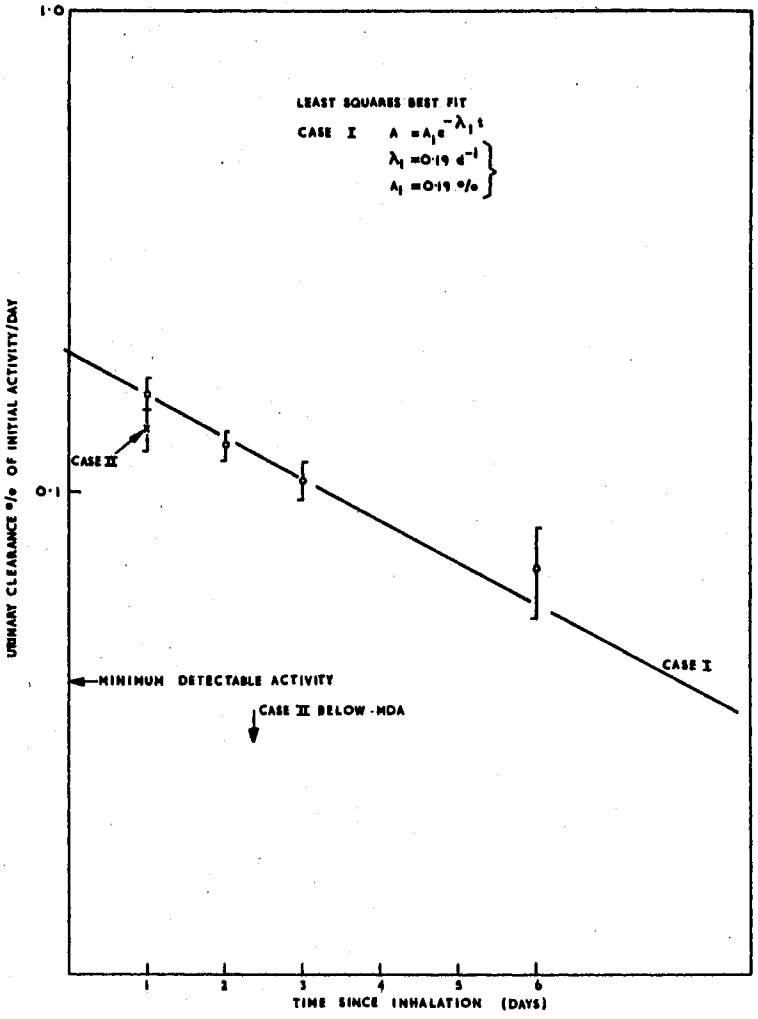

Figure 22. Urinary Clearance of Pu-237 Labelled Particles

with a clearance period of 0.7 days after the peak on day 2. Urinary clearance was negligible only one sample (day 1) being above the limit of detection of the apparatus of 0.04% per day. The isotope accountability, i.e., the sum of retained and excreted fractions, was good in both cases (90%); Figure 23 shows the cumulative fractions retained and excreted together with the totals.

Distribution of Activity

The location of the inhaled activity within the thorax was attempted using a collimated NaI crystal viewing the 100 KeV line. There was insufficient activity present to enable accurate assessment to be made without prohibitively long counting periods. Figure 24 shows results of this exercise and the following broad conclusions can be made.

For Case 1 the deposition (day 1) is fairly uniform throughout the lung initially. The counts are enhanced on day 2 by material moving down the esophagus to the GI tract. After this time the plots show little deposition in the trachea and upper bronchii with long-retained material in the rest of the lung. The efficiency of detection of the 200 KeV line is greater for the middle and upper region because of absorption in liver and other soft tissue of the lower lung gamma emissions. The increase in counts at the base of the lungs is probably significant and does represent enhanced deposition in this area. In Case 2, the initial deposition on day 1 is predominantly in the trachea and upper bronchii regions with rapid clearance of this material via the cilliated epithelium, the esophagus, and the GI tract, which explains the increase in counts over the lower thorax seen on day 2. The residual deposition was just above the limits of detection of the scanning

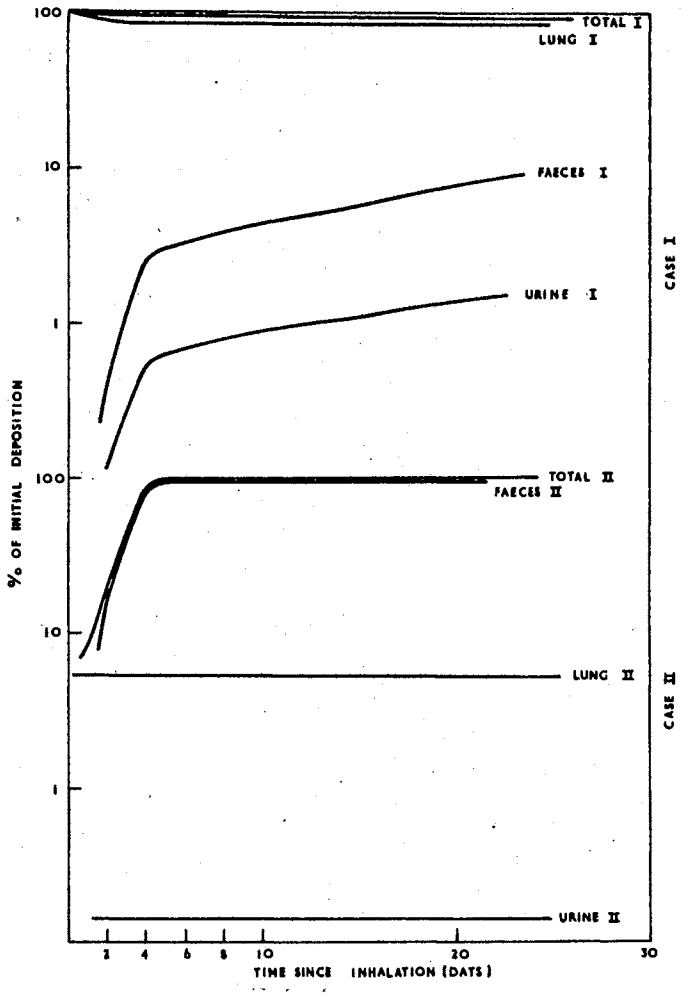

Figure 23. Cumulative Excretion and Retention Fractions

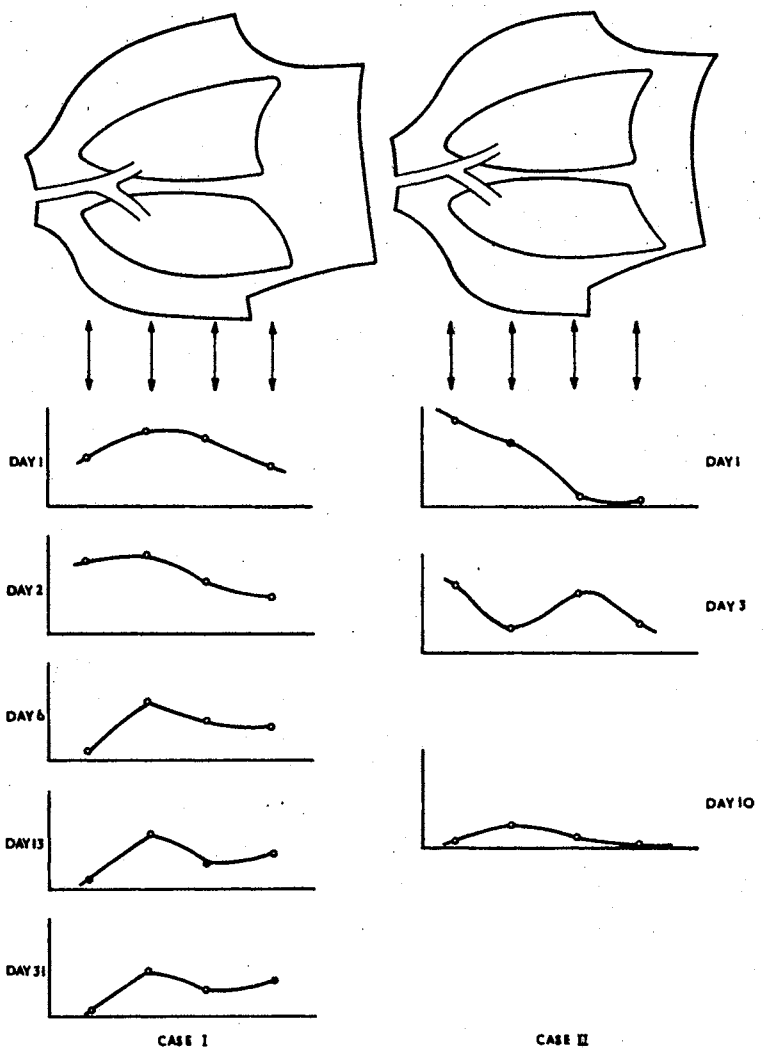

Figure 24. Distribution of Pu-237 Activity in Lungs

equipment and shows slight preferential deposition in the upper lung.

Further wide location studies were made using the 5 in. diameter x 2 in. thick NaI crystal with a one inch steel collimation collar. The efficiency of this detector was higher than the slit collimator, but location could only be attempted to different quadrants of the chest.

In Case 1, the initial deposition was uniformly spread between the two lungs, within 10%, and after the first four days the longitudinal spread, base to apex, was also uniform to within 10%, showing the breathing pattern adopted had given uniform pulmonary deposition. Viewing the lungs from the back of the chest produced higher counting rates than viewing, in a similar geometry, the front of the chest. The magnitude of this effect was 40% and can partially be explained by the presence of the liver and the geometry of deposition and detection. This point is discussed more fully in conjunction with the detection of the L X-radiation (see following page).

Similar measurements of the subject in Case 2 also produced a uniform distribution of residual activity after the clearance of the high initial deposition in the upper thorax. The counting rates from the residual activity from this subject were low, and poor counting statistics were obtained at times beyond four days. There was some evidence of slightly better detection performance with the detector placed below the chest rather than above. This point was more marked at the base of the lungs, probably due to absorption in the liver when the counter is positioned over the base of the right lung.

Using the proportional counter, viewing the 17 KeV X-radiations in a similar way to obtain a crude distribution of deposited activity, Case 1 gave a fairly uniform response both above and below the chest

(± 15%) with peak activities seen above the upper chest and below the lower chest. This effect was again explained primarily by the distribution of absorbing media being predominantly below the upper lung and above the lower lung.

For Case 2 no significant activity was seen below the chest in either position and the peak activity was seen in its upper lung (bifurcation of bronchii) with the counters placed above the chest.

The Detection of the L X-radiations

The raw counting data from the proportional counter measurements of the L X-radiations from Pu-237 were corrected for background; for contributions from the body gamma emitters, i.e., Cs-137 and K-40; and for radioactive decay of Pu-237. In order to express the results as percentages of the initial intake and to compare them with the in vivo data derived from the scintillation detection of the higher energy lines from the inhaled Pu-237 together with the integrated fecal and urinary excretion, it was necessary to derive detection efficiency figures. At these low X-ray energies (13 to 21 KeV) such calibration figures are very dependent on the body build of the volunteer subjects and the sites of deposition of the iron oxide particles within the lung. Appreciable contributions to the counting rate in this X-ray band arise from the scattered and degraded gamma lines at 60 KeV and 100 KeV. These contributions are again very dependent on the scattering medium, i.e., the body build of the subject, and on the choice of gas filling in the proportional counters. In order to get as much information as possible from the measurements, a range of gas fillings was used although a previous study had shown the optimum gas filling for the counters and

electronic system used consisted of a mixture of 66% xenon, 30% argon, and 4% methane (41).

The initial calibration figures were obtained using the Winfrith chest phantom with a series of extended Pu-237 sources placed in the foam rubber lungs (18). These figures were then modified to allow for the gross differences in body build (chest structure) between the phantom and the subjects. A series of ultrasonic measurements of the soft tissue thickness overlying the ribs of a range of normal subjects had enabled the mean soft tissue thickness to be correlated with an expression involving the subject's height, weight, and chest circumference only (17). Using such an expression, the mean soft tissue thicknesses of Subjects 1 and 2 were 2.54 cm and 1.88 cm respectively, compared with 2.00 cm for the chest phantom.

The derivation of this parameter applies only to the area of the chest normally viewed by the proportional counters when used for routine Pu-239 *in vivo* assay, i.e., that area from the third to the sixth rib inclusive. Considering the wide differences in particle deposition observed in these two subjects, the mean soft tissue thickness correction as derived above was considered to be one of the first order only. Differences in calibration efficiency from those derived from the chest phantom would be a combination of geometry differences of detection and differences in mean absorber thickness.

Using the calibration efficiencies calculated from the chest phantom results, the observed data from the proportional counters were expressed as retained percentages of inhaled activity, and lung retention curves were drawn and compared to those obtained by scintillation counting of the higher energy emissions (Figure 20). These are shown

on Figure 25 together with the scintillation detector results taken from Figure 20. In Case 2, the agreement between the 17 KeV detection and the 100 KeV detection was within the quoted errors ($\pm 2\sigma$) for all points and all gas fillings. The proportional counter results gave a simple exponential least-squares-best-fit of 126-day half period and 4.4% initial retained fraction, compared to that of 160 days and 5.4% obtained with the thin crystal. The errors in determining the half period were of the order of $\pm$ 25 days. All proportional counter results were below the corresponding scintillation counter results; the mean ratio of matched pairs being 1.17 is within the errors of measurement. Alternatively this difference could be described as an error of 0.22 cm in the ascribed mean soft tissue thickness (i.e., the same order as the standard error of the estimate 0.2 cm).

In the first inhalation (Case 1) there was no obvious agreement between the initial estimate of lung contents from the proportional counter measurements at 17 KeV and the scintillation counter results at 100 KeV. The two retention curves are also shown in Figure 25. Note also that there was no agreement between the results derived from different gas fillings. The first three points (days 0-3) were obtained with a predominantly argon filling which is relatively insensitive to higher energy radiations and correspondingly more sensitive to errors in assumed mean soft tissue thicknesses. The later results were all obtained with a composite gas filling of 50% argon and 50% xenon and gave good agreement between themselves. The results, as plotted on Figure 25, can be modified by selecting a different mean soft tissue thickness from this subject, reflecting the observed distribution being predominantly deep lung. Such an approach requires a knowledge of the

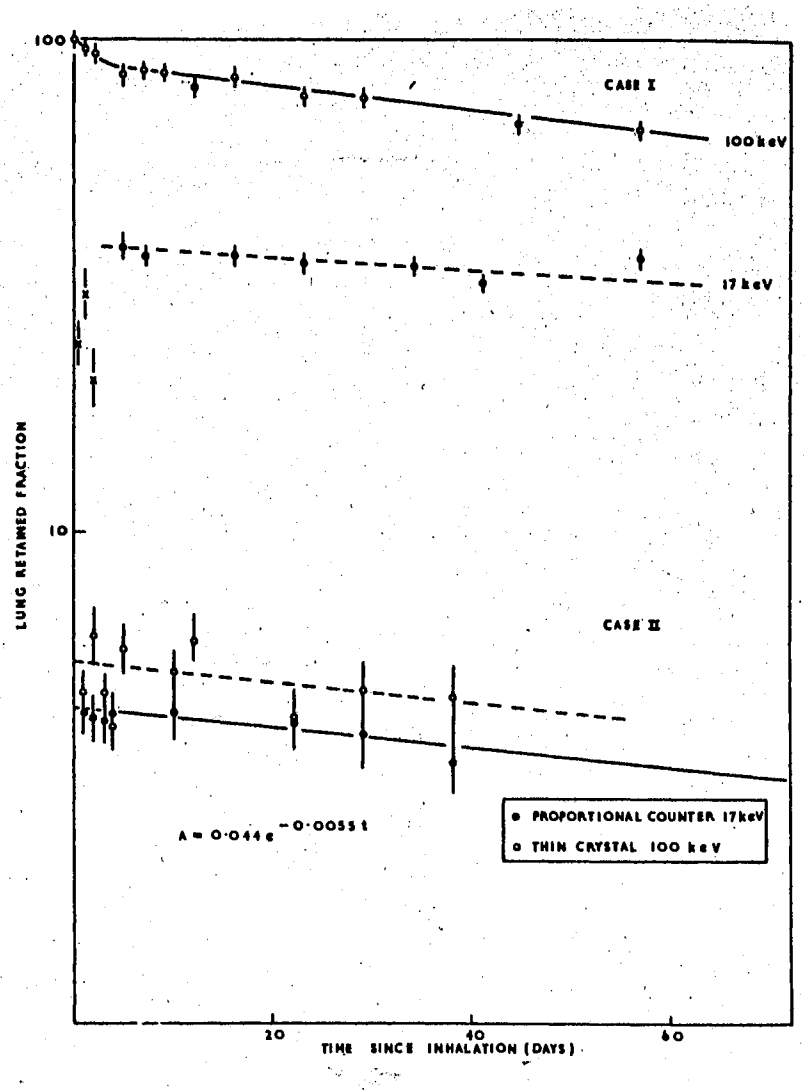

Figure 25. Detection of 17 KeV Radiations

distribution of the different absorbing media, i.e., lungs, muscle, fat liver, ribs, etc., and the analysis would then correct counter response at each energy for absorption, scattering, and geometry of detection.

As a first approach a crude modification of the mean soft tissue factor was calculated, using the observed ratio of the counts obtained from the scintillation detection of the 100 KeV radiations from the front and back of the chest. The observed ratio of 0.71 was then interpreted as both a geometry effect of distribution in the lungs and a corresponding increase in absorbing media above the base of the lungs. The total mean soft tissue thickness from such an approach was 4.0 cm compared with the earlier assumed figure of 2.54 cm. The revised figure was realistic anatomically and in fairly good agreement with the work of Rundo et al.(42). Using such a factor the lung retention points were recalculated and are plotted on Figure 26 together with the thin crystal (100 KeV) data as before. The anomaly between the results from the different gas fillings was no longer evident and the weighted-mean-least-squares analyses of the two retention curves gave a composite curve, as shown of two components of 6 days and 200 days half period with amplitudes of 16% and 84% respectively.

Dose to the Volunteers

In both cases the doses to the lungs of the volunteers were calculated taking the observed deposition patterns and known activity of alpha impurities.

Case 1 total dose to lungs 180 mrems

Case 2 total dose to lungs 13 mrems

Of this dose 85% was due to the alpha impurities. The doses to

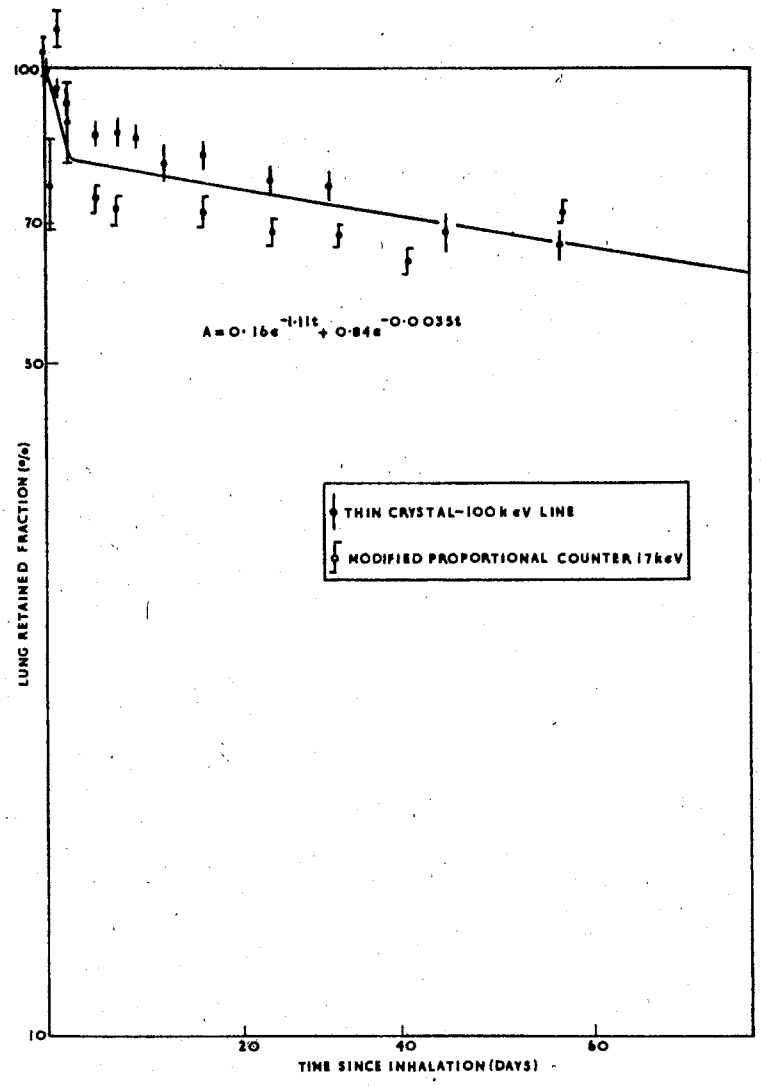

Figure 26. Modified Proportional Counter Data

organs other than the lungs were negligible.

Conclusions

Although the low activity of the tagged particles in the lungs precluded accurate statistical analysis of the data, the retained lung fractions as derived from the detection of the gamma radiations, gave results consistent with the earlier work with Cr-51 and with the I.C.R.P. Task Group on Lung Dynamics(8). The method of approach again demonstrated the feasibility of the technique of doing lung retention studies using minimal amounts of aerosol and activity.

The extrapolation of the data from the detection of the 17 KeV X-radiation to the problem of the detection of Pu-239 *in vivo* revealed that, although the difficulties of low level detection of these radiations is to a large extent overcome, the interpretation of the results in terms of retained lung burdens still posed problems. The approach of using realistic chest phantoms to supply the basic calibration data and attempting to modify such data by body build parameters would appear still to be a valid method but obviously one of first-order correction only. Without such corrections, errors of up to a factor of 10 in calibration would occur.

With the two extremes of breathing pattern chosen for this study the observed errors (using the body build correction factor) were 1.17 and 2.0 for the two cases (note that the error was 4.0 for Case 1 using a gas filling of argon/methane only). In both cases the lung burden of plutonium would have been underestimated. Without some knowledge of the distribution in the lung (i.e., particle size, breathing pattern, length of exposure) following an actual incident, the only check on

validity of the choice of calibration factor would be serial fecal collection to follow observed lung clearance. At low levels of internal contamination when the subject is still working in a plutonium laboratory and probably handling a range of plutonium fuels, such an approach becomes of doubtful validity even if serial fecal sampling were acceptable on other grounds and accurate low-level analysis could be performed.

Although there is little doubt that in an accidental inhalation the particle size distribution and breathing pattern of Case 1 would not be encountered and that the normal in vivo counting procedures in these laboratories would produce an estimate of within 50% of the tissue lung contents even in the case of an atypical exposure, further studies on detection following normal breathing patterns are desirable. A program of work has now been started using more accurate anatomical models to predict the response of the detectors to various distributions of Pu-239 in the lung and to study the feasibility of alternative placing of the detectors around the chest or the use of multi-detector arrays to reduce the uncertainties produced by anomalous distributions of particles within the lung.

CHAPTER VII

CONCLUSIONS AND RECOMMENDATIONS

Because all radiological limits are based on the dose-effect relationship for the irradiation of biological systems, one of the prime considerations in evaluating the potential hazards from internally deposited radioisotopes is the biological dose received by various organs. In such a determination the accurate estimation of the activity intake, A_o, is of paramount importance. Since reconstruction of acute intake is not often possible, the only alternative solution to the problem is the estimation of A_o after the fact by any measure available.

The measures which are available would be better if it were not for the fact that each inhalation and each victim is physically and physiologically different. What is needed, therefore, is a set of data correction factors involving physical and physiological variables. The raw counting or bioassay data could then be treated with the factors to yield an estimate of A_o. Previous attempts have been made to achieve this goal, but the results are limited because of the restriction of related research to laboratory animals or to human phantom studies.

Following an analysis of calibration errors which exist in phantom-related work, an experiment was proposed to minimize these errors. A limited number of experiments were proposed using human volunteers inhaling an aerosol of known activity, solubility, and particle size. Data from the volunteers were to be collected over a definite period of

time by enough independent means to indicate both levels and trends concerning aerosol retention, excretion, translocation, and distribution.

It was decided that the most efficient implementation of these objectives would necessitate: (a) development, construction, and testing of a suitable aerosol generating apparatus; (b) production and investigation of properties of a suitable aerosol; (c) sequential inhalations by a single volunteer of an aerosol tagged first with a soluble form of a gamma-emitting isotope and then with an insoluble form of the same isotope with subsequent compilation of data on the retention, excretion, and distribution of the inhaled material; and (d) inhalations by two volunteers of an aerosol tagged with the insoluble form of an isotope which emits both X-rays in the 13-22 KeV region and gamma rays in the 100-400 KeV region. In these latter inhalations, one volunteer would use a one-deep-breath-and-hold breathing pattern while the other volunteer would use shallow, continuous breathing with the same data being taken as in the previously mentioned inhalations.

Conclusions

Some conclusions which can be drawn from these experiments are:

1. Sub-micron particles generated by ultrasonic nebulization are hollow and have widely varying densities depending upon their size.

2. Excretion, retention, and distribution results following the inhalation of particles generated by ultrasonic nebulization are consistent with ICRP Lung Dynamics Task Group models.

3. The rates and magnitudes of very early lung clearance are independent of the solubility of the inhaled material.

4. Excretion, retention, and distribution characteristics of both soluble and insoluble aerosols can be shown to be identical when the appropriate leaching factors are applied to the data.

5. The inhalation breathing pattern is the primary variable affecting the depth of deposition.

6. The approach of using realistic chest phantoms to supply the basic calibration data and of attempting to modify such data by body-build parameters appears to be a valid method but one of first-order correction only.

7. Without any phantom calibration correction, errors up to a factor of 10 may occur.

Recommendations for Further Work

The collection, analysis, and discussion of these experiments have revealed several worthwhile extensions of this work. This further work might include:

The correlation of these human inhalation calibrations with calibrations of realistic chest phantoms which are in existence.

The extension of phantom work to more accurate anatomical models.

The modification of the inhalation apparatus to make inhalation procedures more automatic.

The extension of the correlation between <u>in vitro</u> leaching and excretion to actual plutonium processing materials.

The investigation of depositions resulting from breathing patterns more nearly normal than the ones used in these experiments.

The investigation of a much greater range of particle sizes and particle solubilities.

The use of the inhalation techniques developed here in the clinical diagnosis of pulmonary disorders.

The improvement of scanning results by using multiple placement of detectors, multidetector arrays, or clinical scanners.

The utilization of more complicated particle shapes in similar investigations.

The multi-isotope scanning of lungs which have inhaled several particle sizes each labeled with unique isotopes.

These recommended extensions would accomplish two very desirable goals. They would apply the knowledge gained to problems existing outside the laboratory and they would extend the knowledge gained to encompass parameters which are more realistic within the laboratory.

SELECTED BIBLIOGRAPHY

(1) Cochran, Terence H. et al. "Liver Injury in Beagles with Pu-239; Distribution Dosage and Damage." Health Physics Journal, Vol. 8 (1962), 699-703.

(2) Stover, B. J. et al. "Further Studies of the Metabolism of Pu-239 in Adult Beagles." Health Physics Journal, Vol. 8 (1962), 589-597.

(3) Dougherty, T. F. et al. "Studies of the Biological Effects of Ra-226, Pu-239, Ra-228, Th-228 and Sr-90 in Adult Beagles." Radiation Research, Vol. 17 (1962), 625-682.

(4) Scott, K. G. et al. "Deposition and Fate of Plutonium, Uranium, and Fission Products Inhaled As Aerosols." Archives of Pathology, Vol. 48 (July 1949), 31-54.

(5) Abrams, et al. "Metabolism and Distribution of Inhaled Pu in Rats." University of Chicago Metallurgical Laboratory Report CH-3655.

(6) Bair, W. J. et al. "Retention, Translocation and Excretion of Inhaled Pu-239 O_2." Health Physics Journal, Vol. 8 (1962), 639-649.

(7) Langham, W. H. et al. "The Los Alamos Scientific Laboratory's Experience with Plutonium in Man." Health Physics Journal, Vol. 8 (1962), 753-760.

(8) Task Group on Lung Dynamics. "Deposition and Retention Models for Internal Dosimetry of the Human Respiratory Tract." Health Physics Journal, Vol. 12 (1966), 173-207.

(9) Hounam, R. F., A. Black, and M. Walsh. "The Deposition of Aerosol Particles in the Nasopharyngeal Region of the Human Respiratory Tract." U. K. Atomic Energy Establishment Report, Harwell, AERE--R 5860, (1970).

(10) Waite, D. A. and B. V. Anderson. "A Projection Chest Phantom for In Vivo Dosimetry." American Industrial Hygiene Association Journal, Vol. 31 (May-June 1970), 322-326.

(11) Dautrebande L. and W. Walkenhorst. "Deposition of Microaerosols in Human Lung with Special Reference to the Alveolar Spaces." Health Physics Journal, Vol. 10 (1964), 981-993.

(12) Rhodes, B. A. et al. "Radioactive Albumin Microspheres for Studies of Pulmonary Circulation." Radiology, Vol. 92 (1969), 1453.

(13) Black, A. and M. Walsh. "Production of Uniform Radioactive Particles for Aerosol Inhalation Experiments--Part I. Particles in the Size Range 1-10 u." U. K. Atomic Energy Establishment Report, Harwell, AERE--R 5716 (1968).

(14) Directory of Whole Body Radioactivity Monitors--1970 Edition. Vienna: International Atomic Energy Agency, 1970.

(15) Peabody, G. O., V. M. Fraser, and R. G. Speight. "The A. E. E., Winfrith, Whole Body Monitor." U. K. Atomic Energy Establishment Report, Winfrith, AEEW--R 215 (1962).

(16) Ramsden, D. "A Multiwire Proportional Counter for the Detection of Pu-239 In Vivo." U. K. Atomic Energy Establishment Report, Winfrith, AEEW--M 526 (1965).

(17) Ramdsen, D., R. T. Speight, and G. O. Peabody. "The Use of Ultrasonics to Investigate Soft Tissue Thickness on the Human Chest." U. K. Atomic Energy Establishment Report, Winfrith, AEEW--R 493 (1967).

(18) Speight, R. G., G. O. Peabody, and D. Ramsden. "An Improved Chest Phantom for Studies of Plutonium and Americium in Human Lungs." Assessment of Radioactivity in Man, Vol. 1. Vienna: International Atomic Energy Agency, 1964, 115.

(19) Ramsden, D. and R. E. Davis. "Unpublished work".

(20) Park, J. F., et al. U. S. Atomic Energy Commission Report, Battelle, BNWL--1050 (1970).

(21) Davies, C. N., Editor. Proceedings of Second International Symposium on Inhaled Particles and Vapors. New York: Pergamon Press, 1967.

(22) Lippmann, M. and R. E. Albert. "The Effect of Particle Size on the Regional Deposition of Inhaled Aerosols in the Human Respiratory Tract." American Industrial Hygiene Association Journal, Vol. 30 (1969), 247-275.

(23) Hanna, M. G., Jr., P. Nettesheim, and J. R. Gilbert, Editors. Inhalation Carcinogenesis. USAEC Division of Technical Information, 1970.

(24) Ramsden D. "The Measurements of Plutonium-239 In Vivo." Health Physics Journal, Vol. 16 (1969), 145-154.

(25) Ramsden, D., M. E. D. Bains, and D. G. Fraser. "In Vivo and Bioassay Results from Two Contrasting Cases of Plutonium-239 Inhalation." Health Physics Journal, Vol 19 (1970), 9-17.

(26) Kanapilly, G. M., O. G. Raabe and G. J. Newton. "A New Method for Generation of Aerosols of Insoluble Particles for Use in Inhalation Studies." Journal of Aerosol Science, Vol. 1 (1970), 313.

(27) Albert, R. E. et al. "Fabrication of Monodisperse Lucite and Iron Oxide Particles with a Spinning Disk Generator." Health Physics Journal, Vol. 10 (1964), 933-940.

(28) Herzog, P., O. P. Norlander, and C. G. Engstrom. "Ultrasonic Generation of Aerosol for the Humidification of Inspired Gas During Volume Controlled Ventilation." Acta Anaesthesiologica Scandinavica, Vol. 8 (1964), 79-95.

(29) Metnieks, A. L. and L. W. Pollak. "Instruction for Use of Photoelectric Condensation Nucleus Counters." Geophysical Bulletin, No. 16, School of Cosmic Physics, Dublin Institute for Advanced Studies, (1959).

(30) Albert, R. E. "Personal communication."

(31) Waite, D. A. and D. Ramsden. "The Production of Experimentally Labelled Aerosols in the Sub-Micron Range," Journal of Aerosol Science, in press.

(32) Brown, C. E. Inhaled Particles and Vapors. New York: Pergamon Press, 1961.

(33) Waite, D. A. and D. Ramsden. "The Inhalation of Insoluble Iron Oxide Particles in the Sub-Micron Range--Chromium-51 Labelled Aerosols." U. K. Atomic Energy Establishment Report, Winfrith, AEEW--R 740 (1971).

(34) Morucci, J. P. Commisariat a l'Energie Atomique Report, CEAR--3027 (1966).

(35) Taylor, B. T. "A Proportional Counter for Low-Level Measurement of Plutonium-239 in Lungs." Health Physics Journal, Vol 17 (1969), 59-69.

(36) Laurer, G. and E. Eisenbud. "Diagnosis and Treatment of Deposited Radionuclides." Excerpta Medica (1968), 189.

(37) Tomitani, T. and E. Tanaka. "Large Area Proportional Counter for Assessment of Plutonium Lung Burden." Health Physics Journal, Vol. 18 (1970), 195-206.

(38) Swinth, K. L. "Diagnosis and Treatment of Deposited Radionuclides." Excerpta Medica (1968), 208.

(39) Rundo, J. et al. "Attenuation in the Chest Wall of 20 KeV X-rays from an Inhaled Radioactive Aerosol." Nature, Vol. 217 (1968), 642-643.

(40) Todd, R. and R. Logan. "Plutonium-237 for Metabolic Studies: Its Preparation and Use." International Journal of Applied Radiation and Isotopes, Vol. 19 (1968), 141-145.

(41) Pike, R. A. and D. Ramsden. U. K. Atomic Energy Establishment Report, Winfrith, AEEW--M 912 (1969).

(42) Rundo, J., K. R. Rudran, and B. T. Taylor. "Effective Tissue Thickness for External Counting of Low Energy Emitters in Lung." Health Physics Journal, Vol. 17 (1969), 155-157.

VITA

David Alan Waite

Candidate for the Degree of

Doctor of Philosophy

Thesis: THE PRODUCTION AND HUMAN INHALATION OF PLUTONIUM LABELLED PARTICLES IN THE SUB-MICRON RANGE

Major Field: General Engineering

Biographical:

Personal Data: Born in El Dorado, Kansas, June 25, 1941, the son of Mr. and Mrs. Noble V. Waite. Married to Nancy Dillingham on August 26, 1962 and father of two sons.

Education: Graduated from El Dorado High School, El Dorado, Kansas, in May, 1959; attended University of Kansas in 1959-1960; received Bachelor of Arts degree from Kansas State Teachers College in 1963 with a major in Physics; received Master of Science degree from Vanderbilt University in 1965 on a Physical Biology Training Grant; completed requirements for the Doctor of Philosophy degree at Oklahoma State University in May, 1972.

Professional Experience: Asst. Prof. and Head, Department of Radiation and Nuclear Technology, Oklahoma State University, 1965-70; Summer Scientist, Battelle Northwest Laboratory, Summers of 1967-68; Attached Staff, Radiological and Safety Division, Atomic Energy Establishment, Winfrith, Dorset, England, 1970-71; President and Chief Consultant, Radiation Services and Consultants, Inc., October 1968 to present.

Professional Organizations: Sigma Pi Sigma, Lambda Delta Lambda, Health Physics Society, Society of Nuclear Medicine